Open access • Journal Article • DOI:10.1039/C6EE01137C

Progress, challenges and perspectives in flexible perovskite solar cells

Francesco Di Giacomo, Azhar Fakharuddin, Azhar Fakharuddin, Azhar Fakharuddin ...+2 more authors

Institutions: University of Rome Tor Vergata, Quaid-i-Azam University, Universiti Malaysia Pahang, University of Konstanz

Published on: 05 Oct 2016 - Energy and Environmental Science (Royal Society of Chemistry)

Topics: Roll-to-roll processing

Erschienen in: Energy & Environmental Science ; 9 (2016), 10. - S. 3007-3035
https://dx.doi.org/10.1039/c6ee01137c

Energy & Environmental Science

REVIEW

Cite this: Energy Environ. Sci., 2016, 9, 3007

Progress, challenges and perspectives in flexible perovskite solar cells†

Francesco Di Giacomo,‡[ab] Azhar Fakharuddin,‡[cde] Rajan Jose[c] and Thomas M. Brown*[a]

Received 18th April 2016,
Accepted 12th August 2016

DOI: 10.1039/c6ee01137c

www.rsc.org/ees

Perovskite solar cells have attracted enormous interest since their discovery only a few years ago because they are able to combine the benefits of high efficiency and remarkable ease of processing over large areas. Whereas most of research has been carried out on glass, perovskite deposition and synthesis is carried out at low temperatures (<150 °C) to convert precursors into its final semiconducting form. Thus, developing the technology on flexible substrates can be considered a suitable and exciting arena both from the manufacturing view point (*e.g.* web processing, low embodied energy manufacturing) and that of the applications (*e.g.* flexible, lightweight, portable, easy to integrate over both small, large and curved surfaces). Research has been accelerating on flexible PSCs and has achieved notable milestones including PCEs of 15.6% on laboratory cells, the first modules being manufactured, ultralight cells with record power per gram ratios, and even cells made on fibres. Reviewing the literature, it becomes apparent that more work can be carried out in closing the efficiency gap with glass based counterparts especially at the large-area module level and, in particular, investigating and improving the lifetime of these devices which are built on inherently permeable plastic films. Here we review and provide a perspective on the issues pertaining progress in materials, processes, devices, industrialization and costs of flexible perovskite solar cells.

Broader context

For a number of years, solar cells had been considered as an inferior energy technology due to high cost – even in the renewable energy paradigm; however, more recently progress in materials processing and engineering of highly efficient and stable solar panels have helped them emerge as a frontline renewable energy technology with energy payback time that has been lowered from over a decade to a couple of years (at least in some parts of the world) during the last ten years. Commercial solar panels are typically manufactured on rigid platforms. Fabricating them on flexible substrates, such as transparent plastics and metallic foils, would enable effective harvesting of energy in a number of diverse areas from indoor electronics to automobiles and from building integrated photovoltaics to portable applications. Furthermore, it would open up web-based roll-to-roll fabrication conducive to massive throughputs. Solution processable perovskite solar cells offer promising opportunities towards this end. Being these cells the most efficient among the solution processable ones, with efficiency in their laboratory scale devices on par with the commercially available silicon and thin film counterparts, significant recent efforts devoted to their manufacturing on flexible substrates have seen efficiencies rise as high as 15.6% together with moderate stability. We approach the developments in this area by critically analyzing the factors affecting the final performance indicators such as efficiency, stability, and functionality and relate these to its processing parameters. We identify the emerging processing trends in this area and critically comment on the needs to develop them as a deployable device.

1. Introduction

Energy harvesting remains one of the biggest challenges of mankind for the future.[1] Renewable energy sources, such as solar and wind, need to take up an ever growing share of energy demand which today is still largely fulfilled by fossil fuels.[2] The sun alone transfers ~120 000 TW of power to the earth, compared to the current global need of ~17 TW.[3] To harness this potential, solar cell technologies are poised to shape future energy trends.[4] Photovoltaic (PV) installations worldwide have surged from ~805 MW in 2000 to ~175 305 MW in

[a] C.H.O.S.E. (Centre for Hybrid and Organic Solar Energy), Department of Electronic Engineering, University of Rome Tor Vergata, via del Politecnico 1, Rome, 00133, Italy. E-mail: thomas.brown@uniroma2.it
[b] Holst Centre/TNO - Solliance, PO Box 8550, 5605 KN Eindhoven, The Netherlands
[c] Nanostructured Renewable Energy Materials Laboratory, Faculty of Industrial Sciences and Technology (FIST), Universiti Malaysia Pahang, 26300 Kuantan, Malaysia
[d] Nanosciences and Technology Department, National Center for Physics, Quaid-i-azam University, Islamabad, Pakistan
[e] Department of Physics, University of Konstanz, D-78457, Konstanz, Germany

† Electronic supplementary information (ESI) available. See DOI: 10.1039/c6ee01137c

‡ Both authors have contributed equally to this work.

2014 increasing from ~0.1% to ~9.6% of total renewable energy installations respectively.[5]

PV devices can be classified in three types, first generation PV (*e.g.* crystalline silicon), second generation thin film PV (*e.g.* amorphous silicon, cadmium indium gallium selenide (CIGS) and cadmium telluride (CdTe))[6] and new generation PV.[7] Examples of the latter are dye-sensitized solar cell (DSCs), organic photovoltaics (OPVs), quantum dot solar cells (QDSCs) and, recently emerging, perovskite solar cells (PSCs).[8–10] By the end of 2015, silicon solar cells (wafer technology) dominated taking up ~90% of the PV market followed by ~9% for thin film counterparts.[11] With power conversion efficiencies (PCE) of commercial modules of around 20% (and ≥25% in laboratory cells[12]) and stability >20 years, c-Si has progressed in achieving grid parity in well-sunlit regions.[13–16] In fact their cost, partly also due to the oversupply in market, has dropped significantly from ~70$ per W_P in the 1970s to ~0.7$ per W_P in 2014.[17] The energy payback time (EPBT) has also decreased to ~2.5–3 years.[11]

Although much R&D is trying to push numbers like cost per Watt peak and energy pay-back time down further, it is the new generation PV which is aiming for breakthroughs on that front (*e.g.* EPBT < 0.5 years and cost <0.5$ per W_P). In fact all new generation PV technologies mentioned above are being developed with low-cost, large-area deposition techniques, cheap materials and less-energy intensive processes. However, with the strong progress made by c-Si in the last decade it is difficult for new technologies aiming to enter the market to compete

Published on 09 September 2016.

Francesco Di Giacomo

Francesco Di Giacomo received his MSc degree in Material Science and Technology from the Tor Vergata University in Rome, Italy. He investigated the upscaling of perovskite solar cells on rigid and flexible substrate during his PhD at the Centre for Hybrid and Organic Solar Energy (CHOSE) of the University of Rome – Tor vergata. He recently joined the Holst Centre – Solliance as a research scientist and is mainly involved in the development of sheet-to-sheet and roll-to-roll production of perovskite solar cells and modules via slot-die coating. He is author of 12 publications on perovskite solar cells and modules, including first flexible perovskite module. E-mail: francesco.digiacomo@tno.nl

Azhar Fakharuddin

Azhar Fakharuddin holds a PhD in Advanced Materials from the Universiti Malaysia Pahang where he worked on nanomaterials for dye-sensitized solar cells. He has also been attached to the Centre for Hybrid and Organic Solar Energy of the University of Rome Tor Vergatta to carry on his research in perovskite solar cells and modules. He is currently an Alexander von Humboldt Postdoctoral Research Fellow at the Department of Physics of the University of Konstanz, Germany where his work mainly includes interface engineering of perovskite solar cells and also its long term stability. E-mail: Azhar.fakhar@yahoo.com or Azhar-fakhar.uddin@uni-konstanz.de

Rajan Jose

Rajan Jose is a Professor of Materials Science & Engineering at the Faculty of Industrial Sciences & Technology, Universiti Malaysia Pahang (UMP) since 2010. He did his doctoral research at the Council of Scientific & Industrial Research (CSIR), India and received PhD degree in 2002. He supervises the Nanostructured Renewable Energy Materials Laboratory in the UMP. He has worked at the Indira Gandhi Centre for Atomic Research (India), AIST (Japan), Toyota Technological Institute (Japan), and the National University of Singapore (Singapore) before joining UMP. He is a materials engineer with most of his research on the structure–property correlation in materials for a desired device functionality. E-mail: rjose@ump.edu.my

Thomas M. Brown

Thomas M. Brown investigated polymer OLEDs for his PhD at the Cavendish Laboratory, University of Cambridge. From 2001–2005 he developed OTFTs and E-paper as Senior Engineer with Plastic Logic Ltd. In 2005 he was recipient of a "Re-entry" Fellowship awarded by the Italian Ministry of University and Research and is Associate Professor at the University of Rome-Tor Vergata. Cofounder of the Centre for Hybrid and Organic Solar Energy, his current research is in solution-processed solar cells including perovskites, especially on flexible substrates. He is author of over 100 publications and 16 patents and is associate editor of Solar Energy. E-mail: thomas.brown@uniroma2.it

directly with c-Si on the conventional PV system market. Thus, technologies such as DSCs and OPVs that have been researched for over two decades, whilst demonstrating lower PCE (of the order of 12–14% in laboratory cells), are now being developed industrially to compete on markets where their added functionalities can deliver properties which c-Si cannot easily, such as transparency, color/shape control, high performance under diffuse or indoor light, and flexibility,[18] making them suitable and very interesting initially for building-integrated, automotive or for light weight portable or indoor applications.[7]

Perovskite solar cells are a much more recent PV discovery. They have attracted huge interest because they promise to combine the benefits of high efficiency (today above 20% on small lab cells)[19–23] and 11–13% over small module areas,[24–26] and the remarkable ease of processing over large areas at low temperatures typical of organic PV (*i.e.* for improved \$ per W_P values and EPBT). PSCs were first reported in 2009 by Kojima *et al.*,[27] who employed hybrid metal halide perovskites ($CH_3NH_3PbI_3$ and $CH_3NH_3PbBr_3$), previously used in optical devices and field-effect transistors,[28–30] to replace the organic sensitizer in a DSC, and obtained a PCE ~ 3.8%. However, presence of the liquid electrolyte dissolved the perovskite crystals over time leading to a drastic degradation. Research in PSCs showed a surge after reports by Kim *et al.*[31] in 2012, who replaced the liquid electrolyte with a solid-state hole conducting material depositing the perovskite precursor over the mesoporous TiO_2 layer achieving a PCE of 9.7% and by the research group of Prof. Snaith, who demonstrated that efficient PSCs can be fabricated by substituting the mesoporous TiO_2 with an insulating Al_2O_3 scaffold (PCE ~ 10.9%), or even without any mesoporous structure (planar architecture, PCE ~ 12.3%).[32,33] The research group of Prof. Gratzel, inspired by the pioneering work of Mitzi *et al.*,[33] demonstrated a sequential deposition to produce pinhole free perovskite layer that showed a large increase in PCE (~15%).[34,35] The subsequent 3 years demonstrated a dramatic rise in increasing the PCE of these devices, with over 1500 publications reported to date, with the optimization of materials, device architectures and interfaces, resulting in PCEs 20–22%.[19–23] Even though questions about their outdoor stability, particularly when exposed to humidity,[36–38] UV-light[39] and high temperatures[40,41] still need to be comprehensively answered, various commercial companies such as Oxford PV, Dyesol, G24 power are actively involved in developing large scale fully printable PSCs. Oxford PV has announced its commercial roadmap with first delivery anticipated in 2017–2018 and investments of over ~£13 million in 2015.[42] Such rapid push for industrialization, merely a few years after their discovery, has been enabled primarily by the fact that deposition and processing facilities that had been developed for DSCs and OPVs can be implemented for PSCs since most of the fabrication processes are similar.

PSCs have mostly been developed over glass substrates, both as laboratory cells and as larger area modules.[43,44] There has also been interest, as a candidate for a possible initial commercial deployment, in incorporating a top ~1 μm thick perovskite subcell in a tandem device with a silicon subcell or a CIGS based thin film device in order to further reduce the cost-efficiency balance of the technology.[45] The tandem configuration should be able to increase the PCE by 20% (bringing it to over 30% in absolute terms)[46] but the best published reports are still well below this target.[46–51]

Apart from the high PCEs delivered, the key advantage of this new PV technology consists in the possibility of relatively simple processing of the perovskite precursors either *via* vapour techniques or in solution (*i.e. via* printing techniques) requiring low temperatures to convert into their final semiconducting form (<150 °C).[52] When low temperature processing is also developed for the charge extraction layers, scaffolds (where present) and electrodes, processing temperatures below the 150 °C threshold permit the fabrication of this solar technology on transparent plastic films[53] such as polyethylene terephthalate (PET) or on conductive indium tin oxide-coated PET/ITO sheets or rolls. Flexible conducting plastic films and metallic substrates can be potentially made cheaper than the conducting glass counterparts.[54] Importantly, developing perovskite photovoltaic module technology on thin flexible plastics permits rapid web-based reel-to-reel manufacturing and potentially massive product volumes and throughputs thus contributing to cutting industrial costs.[18]

Developing the technology on plastics brings about a series of non-trivial challenges and issues related to the nature of the substrates which are not present on glass substrates (*i.e.* distortions, low temperature processing only). The highest reported PCEs of small flexible laboratory PSCs (f-PSCs) are, in fact, still significantly lower than glass based PSCs, *i.e.* 14–15%[55,56] with the highest being 15.4–15.6%.[57] Nevertheless, these values can be considered very promising as they are significantly higher than other new technologies such as OPV and DSC for which highest PCEs are in the 11–14% range even when fabricated on glass.[58,59] There is however ample scope to close the glass–plastic gap in the future, especially regarding the development of large area modules where the literature is limited. Deployment of flexible PV technology is not only motivated by the quest for high-throughput and low-cost manufacturing but also by the markets it would be able to access considering its properties (of being flexible, thin, lightweight) would make it easy to integrate or apply on any surface (*e.g.* BIPV, AIPV) or structure (either rigid, curved or flexible) and even in portable and indoor electronics. Furthermore, one can exploit its 3D conformability considering that over the course of a day, curved cells outdoors have been shown to deliver more energy over their footprint projected area compared to flat ones.[60]

Here we review the progress in this exciting field related to the development of flexible perovskite solar cells. Purpose of the following Sections 2 and 3 is to provide a brief overview of the PSCs and the current state of affairs of the flexible PV technology for a better understanding of this article. Section 4 of this article provides an overview of the varied choice of flexible substrates employed in the PV technology. Sections 5 and 6 review the literature on f-PSCs fabricated on transparent conducting oxide TCO/plastic substrates with bottom electron

or hole transport layers respectively. Section 7 covers TCO-free device whereas Section 8 those manufactured on metal foils. Section 9 describes efforts in upscaling the technology over large areas and flexible modules. Section 10 extends the discussion to low temperature processing and deposition techniques over large areas that are applicable to this technology. Section 11 reviews the investigations carried out on stability whereas Section 12 introduces some cost and life cycle analyses. Section 13 provides a perspective on the publication and patent output internationally over the years. Section 14 finishes with conclusions and outlook.

2. An overview of perovskite solar cells technology

Readers are referred to the ESI† of this article for an overview of perovskite crystal structure, its optical and electronic properties, working mechanisms and different device fabrication methods. More details can be found in many reviews published on this topic.[45,61–63] Briefly, perovskite stands for a class of materials with crystal structure defined by ABX_3, where ''B'' is 6-fold anion ''X'' coordinated, thereby making BX_6 octahedra, and ''A'' is another cation with 12-fold ''X'' coordination (see Fig. S1, ESI†).[45] Perovskites provide an array of physical properties such as piezo-, ferro-, and pyro-electricity;[64] the range of electrical properties of perovskites is probably the widest physical property exhibited by a single class of material (from dielectrics to superconductivity). Most of the above are purely inorganic (mostly oxides). Recently, hybrid perovskites containing both organic and inorganic components in the unit crystal have come to the fore showing remarkable performance as semiconductors (solar cells, LEDs and even TFTs) when integrated in optoelectronic devices as thin polycrystalline films. Methyl ammonium lead iodide ($CH_3NH_3PbI_3$) is the organic–inorganic hybrid perovskite under focus for the PV applications due to its desirable band gap (1.55 eV),[61] its high absorption coefficient (10^3 cm^{-1}) and low exciton binding energy allowing the film thickness to be <500 nm to collect most of the incident light (see Fig. S2, ESI†),[45] and high electron- and hole-diffusion lengths (up to 175 μm for single crystals) enabling even planar heterojunction configurations.[65]

Perovskite crystal structure also offers diversity to accommodate various chemical entities (either atoms or atomic groups) meeting size and charge balances such as Cs^+ and formamidinium $CH(NH_2)_2^+$ at the A-site, other halogens (*e.g.* Br) at the X-site when Pb is maintained at the B-site. Chemical substitution allows one to tailor the band gap of the perovskite semiconductor (see Fig. S3, ESI†). The $CH_3NH_3PbI_3$ films can be simply solution processed by allowing its precursors (*e.g.* PbI_2 + CH_3NH_3I) dissolved in an aprotic polar solvent (such as DMF) to crystallize on a substrate/electrode.[66,67] The PSCs could be fabricated by sandwiching the $CH_3NH_3PbI_3$ films between two charge selective contacts (see Fig. S4, ESI†), *viz.* hole transport material (HTM) and electron transport layer (ETL). Absorption of light promotes electrons from the perovskite valence band to the conduction band. The weakly-bound exciton, splits into free charges, and thus PSCs are better represented by a free carrier model. The electrons and holes can thus drift-diffuse towards the selective contacts and the electrons are finally extracted at the electrode/ETL on one side and the holes at the electrode/HTM on the other. Effective ETLs and HTMs possess energy levels which block the other type of carrier thus minimizing recombination (see Fig. S4, ESI†). If the perovskite is coated on the ETL, the structure is called n–i–p or direct or regular, while cells with perovskites coated on the bottom HTL are called p–i–n or inverted structures (see Fig. S5, ESI†).[61] The synthesis of the perovskite thin-films is generally achieved by reacting a lead halide salt with a methylammonium halide salt. There are two main approaches to perform and control this reaction: single-step and double-step (also called sequential deposition method). Solution processing is most widely used where the precursors are dissolved in solvents (together in the single step and deposited sequentially separately in the double step) and deposited *via* spin coating or other coating/printing techniques but thermal evaporation of the precursors or of the whole perovskite has also been demonstrated. The deposition methods, ink formulations (or evaporation parameters) and the underlying substrates/transport layers determine the degree of crystallinity, homogeneity, and morphology of the thin films (see Fig. S6, ESI†) which have a strong bearing on solar cell efficiency and stability. Because the choice of the bottom charge selective contact influences the growth of the perovskite layer deposited on its top, as well as providing different materials and manufacturing challenges, the n–i–p (*e.g.* substrate/TCO/ETL/perovskite/HTM/Au) and p–i–n (*e.g.* substrate/TCO/HTM/perovskite/ETL/Au) architectures will be treated in separate sections. An additional classification is related to the morphology of the selective contact, which may be either mesoscopic (*e.g.* substrate/TCO/compact-TiO_2/mesoporous-TiO_2/perovskite/HTM/Au containing a nano-crystalline scaffold) or planar (*e.g.* substrate/TCO/ETL or HTM/perovskite/HTM or ETL/Au with no scaffold) where the transport layers can either be inorganic such as metal oxides TiO_2 (ETL), ZnO (ETL), NiO_x (HTM) or organic such as Spiro-OMeTAD (HTM), PTAA (HTM), PEDOT:PSS (HTM), PCBM (ETL). The use of a triple stack of mesoscopic layers (ETL, spacer and carbon electrode) has led to the design of a fully mesoporous PSC.[68] Each architecture has pros and cons when implemented over a flexible substrate, and a detailed discussion will be given in Sections 4–8.

3. Flexible PV technologies

In order to better understand and evaluate the potential of f-PSC, it is worth briefly summarizing the state-of-the-art of flexible PV technology in more general terms. Whereas first generation PV based on monocrystalline semiconductors is intrinsically rigid, the emergence and evolution of thin film (second generation) and new generation PV (manufactured *via* solution processing and/or evaporation techniques) with good intrinsic flexibility has seen greater efforts dedicated to the development of solar cells on flexible substrates. The absorption

coefficient of crystalline Si, an indirect band gap semiconductor, is rather low. Therefore, relatively thick wafers are required both to guarantee efficient absorption over the whole spectral range as well as sufficient mechanical stability (since these must be self-supporting until placed inside a module). By reducing the thickness of the Si wafer it is still possible to fabricate semi-flexible modules with high efficiency ($\sim$15–20%); however, bending radius $<$10 cm induces damage to the module.[69] To overcome the brittleness of large Si crystalline wafers, new concepts have been developed. The Si wafer is structured in very thin (1–2 mm) electrically-interconnected stripes allowing to dramatically reduce the bending radius to the cm scale without large decreases in PCE (module efficiency $\sim$18.3%).[70,71] However, the additional dicing step and the high precision required in the manufacturing increases manufacturing cost.

The highest efficiencies for flexible solar cells, so far, have been reported by Alta Devices with cells based on GaAs fabricated with a lift-off process. This allows to manufacture the cell on a heat-resistant GaAs single crystal by metalorganic chemical vapour deposition (MOCVD) and then transferring the stack on a flexible substrate, obtaining efficiencies of up to $\sim$26.7%.[72] The reduced thickness of GaAs solar cells compared to c-Si[73] makes this technology more suitable for flexible substrates;[73] however, the high price of multi-junction GaAs solar cells limits their use in applications such as outer space, where the cost is not a limiting factor, or in concentrators, where flexibility is not a requirement.[74]

Thin-film PV represents a more suitable option for large area production of flexible modules thanks to the intrinsic bendability of the active layer given by the reduced thickness. Amorphous silicon can be deposited on flexible substrates and cells based on a-Si:H/a-SiGe:H/nc-Si:H multi-junctions exhibited efficiency of up to 16.3% (12.5% stabilized), very similar to the rigid equivalents.[70,75] In the case of CdTe solar cell the gap between rigid and flexible cells is larger due to the high temperature usually required for fabrication. If the efficiency of rigid devices can go up to 22.1%, on flexible glass substrates the efficiency is lowered to 16.4% and the relatively high price and the brittleness of flexible glass make them less attractive for a number of large area applications together with limits on the bending radius.[76] CdTe can be also produced on polyimide films, but the efficiency is reduced to 13.8% due to the processing temperature limited to 450 °C.[77] Higher temperatures can be used on metal foil, but the PCE is still limited to 13.6%.[76,78] On the other hand, flexible CIGS cells reached very high PCE, similar to the rigid equivalent. The record for flexible CIGS is 20.4% on polyimide foil, only 2% lower than the one for glass based cells.[79] The reduction of the maximum processing temperature to values lower than 450 °C ease the transfer of the fabrication procedures from glass to temperature resistant flexible substrates such as polyimide. These efficiency values may make flexible devices an attractive replacement for both bulk energy productions in large solar plants and in BIPV.

New generation PV such as OPV and DSC lowers the thermal budget needed to fabricate flexible devices, enabling the use of low cost PET polymer film. DSCs on glass are usually prepared at high temperature (450–500 °C) to sinter the mesoporous TiO_2 layer. For this reason, research on flexible DSCs has been divided among groups focusing on metal substrates (mainly Ti) and on PET/ITO films.[18] For PET/ITO it has been necessary to develop low temperature processes, while metal foils allow the use of conventional high temperature processes but the amount of light reaching the active dye sensitized layer is reduced by absorption through the non-transparent electrolyte. The maximum efficiencies reached with flexible DSCs are 8.1% and 8.6% for PET/ITO and metal substrate respectively under standard test conditions,[80,81] currently limiting the application of such cells to indoor light harvesting where the performance was found to be higher than for other PV technologies.[82] OPV has probably been the most suitable technology for development on flexible substrates up to now due to the low temperature ($<$150 °C) required for fabrication. Most academic research has focused on solution processing, and feasibility of roll-to-roll manufacturing has also been demonstrated.[83] Furthermore, by introducing the use of organic electrodes based on PEDOT:PSS, organic semiconductors have been implemented in stretchable PV devices, enabling the use of flexible PV in new applications.[84] The very low temperature needed allows one to work on ultrathin substrates, and, before the development of f-PSCs, OPV held the record for power/weight ratio in PV technologies.[84,85] Rather than with solution processing, the highest efficiencies obtained in OPV have been based on vacuum evaporation of small molecules by Heliatek. The company claimed efficiencies of up to 13.2% on glass/ITO for their multijunction cells and up to 10% for flexible modules with an ITO-free production-feasible stack. They also have facilities to produce large area modules *via* vacuum roll-to-roll manufacturing with efficiencies of up to 7.7% for a stack that yields similar results in the lab.[86]

Flexible PSC will compete with all these technologies, but has, and can also continue to, use the know-how generated by them. For the planar architectures in which a f-PSC resembles a flexible organic solar cell (*i.e.* low temperature processing, deposition from solution or evaporation, being lightweight and compatible with stretchable substrates), benefits arise from higher efficiencies (true at the small laboratory flexible cell level at the moment) that can aim to reach the ones of CIGS. Most of the coating techniques and several selective contacts used for OPV can be used by f-PSCs, as well as the roll-to-roll facilities developed so far. With respect to f-CIGS cells, lower processing temperature of perovskite films allow the use of cheaper and potentially more transparent substrates, and one can surmise that the efficiency gap between glass and f-PSC could become even lower than for CIGS in the future. Essential know-how can be obtained from DSC research, especially for the mesoporous architecture, and also from thin-film technologies which have already developed large area processes to deposit TCO and laser interconnections. Effective encapsulation is also a common issue for all these flexible PV technologies where resources should be pooled. As a closing remark, in order to increase the maximum efficiency of cost-effective

flexible solar cells, fabrication of flexible tandem cell based on CIGS and perovskite is proposed to be a viable concept to reach efficiency ~25%, a value that also would allow to compete with silicon for the realization of large solar plants.[87]

4. Flexible perovskite solar cells and choice of substrates

Most of the efforts of academic and industrial research have been focused on the development of PSC on rigid glass substrates. Nevertheless, research on flexible PSCs is growing rapidly, with the highest PCE reported of 15.4–15.6% for planar cells on plastic substrates using a compact ZnO layer.[57] Similarly to other thin-film or OPV solar cells, PSCs can be bent down to millimetre scale radius, and are characterized by low weight.[88] As mentioned in the introduction, these features make it an ideal choice for the energy harvesting of portable devices or for any application in which the energy source should be conformed to a curved surface like in building-integrated photovoltaics.

Besides the applications which require the flexibility of the device, flexible substrates enable to implement roll-to-roll fabrication, with an opportunity to improve the production throughput and to reduce manufacturing costs.[89] Amorphous-Si, CIGS and CdTe thin-film solar cells, due to the relatively high process temperatures, are usually fabricated on polyimide plastic films or on metal foil. Efficiencies of 16.3% have been reported in triple junction amorphous silicon devices on polyimide, 13.6% in CdTe on metal and 20.4% in CIGS on a polyimide.[18] For PSCs, thanks to the lower processing temperature needed, the more transparent and lower cost polyethylene terephthalate (PET) polymer is often used, similarly to the Dye Solar Cell and OPV fields.[90]

Indeed PSCs have already delivered very high efficiencies using low temperature processes (below 150 °C) on glass substrates, with PCEs of up to 19.3%.[91] The active material itself is always processed at temperatures compatible with plastic substrates (well below 150 °C). This is also true for the top selective contact, which is deposited already with techniques that do not require or lead to high sample temperatures. On the other hand, high temperature processes are often used to fabricate the metal oxide bottom layers which are used to collect carriers and avoid recombination with the substrate. Thus, much of the efforts in developing flexible PSC are focused on developing alternative materials and/or low temperature processes for such layers.

A strategy to overcome temperature-related issues is to use a metal substrate that additionally has good barrier properties. The use of metal or polymeric substrate strongly influences the processing of the devices. For instance, high temperature processes cannot be used on polymeric film, while a semi-transparent top contact is mandatory on a metal substrate. For this reason the examination of the state of the art of flexible PSC will be split in two main sections, one on PSC on polymeric film and one on PSC on metal foil.

Films of PET and polyethylene naphthalate (PEN) are widely used as transparent and lightweight substrates for PV applications.[53] In order to use them as a transparent electrode substrates, they are typically coated with transparent conducting oxides (TCO) such as indium tin oxide (ITO) or similar materials like indium zinc oxide (IZO) or aluminium doped zinc oxide (AZO), in some cases with the addition of an ultrathin silver layer.[53,92,93] The sheet resistance of these ITO/polymer substrates reaches 10–15 $\Omega\ \square^{-1}$, relatively close to the typical value of TCO-coated glass used for PV applications (7–15 $\Omega\ \square^{-1}$) retaining good transmittance in the visible spectrum, at lower costs. Beside their good transparency/conductivity, plastic/ITO substrates are characterized by several issues. Firstly, ITO is a brittle material, so it can be damaged during bending, leading to increase in substrate resistance and propagation of cracks in the active layers.[94] Nevertheless, it is sufficient to avoid curving devices below the safe bending radius of ITO (that depends on the ITO thickness) to prevent any degradation from occurring. For instance, it has been shown that the safe bending radius for PET/ITO, with sheet resistance of 15 $\Omega\ \square^{-1}$, is equal to 14 mm.[53] Secondly, ITO layers that are annealed at low temperatures show reduced chemical resistance with respect to crystalline ITO or FTO, especially in acidic solution, and may induce degradation in the perovskite film if they are not carefully covered by pinhole-free compact layers. The different quality of the ITO deposited on glass or polymer film partly explains the higher PCE typically obtained on glass-ITO with respect to PET-ITO, even when the same fabrication process is employed.[95]

Additional thermal constraints arise because of the substrate itself. In order to use a PET or PEN film as a substrate, a low temperature fabrication process must be developed ($T < 150$ °C). This might be initially an issue in the fabrication of PSCs with a n–i–p architecture, since it usually requires an n-type metal oxide sintered at high temperature. On the other hand, in the inverted (p–i–n) planar architecture all materials are typically processed at low temperatures. A way to overcome the temperature limitation is to use an ultrathin flexible sheet of glass. The only article that uses the latter for a PSC will be discussed in the next section. However, the brittleness and high cost of ultra-thin glass are still preventing its application on large scale. For the sake of a clear description of the state of the art, the n–i–p and p–i–n structures will be treated in two distinct sections. Later on, an additional section will discuss the use of polymer films without TCO, where an organic layer based on PEDOT:PSS (with or without a metal grid) or carbon nanotubes (CNT) was used as the transparent conductive electrode.

5. Flexible n–i–p PSCs with compact electron-extracting layer on TCO/plastic substrates

In PSCs with conventional n–i–p architecture, the first layer deposited on the TCO is an n-type layer. Its function is to

extract the photogenerated electrons form the perovskite, transport them to the TCO and avoid recombination between perovskite and TCO by blocking holes. To fulfil these requirements, these layers should be ideally pinhole-free (indeed they are also known as compact layers), should provide a suitable electron affinity for electron extraction and should possess high electron mobility. Furthermore, a high ionization potential can also guarantee good hole blocking properties. Even if there are reports on flexible and rigid PSCs with no compact layer displaying high PCEs with a fast JV scan,[96,97] the steady state PCE measured is close to zero, confirming the requirement for this layer.[98]

Wide band gap metal oxide semiconductors such as TiO_2, ZnO and SnO_2 are ideal and most-commonly used candidates as ETLs as a result of appropriate energy levels (see Fig. S4, ESI†). Both TiO_2 and ZnO have a conduction band (CB) that lies approximately at 4–4.2 eV from the vacuum level, suitable for efficient electron extraction (CB of $CH_3NH_3PbI_3$ is at 3.9 eV from the vacuum level).[61] Nevertheless, it is important to notice that especially when low temperature fabrication procedures are employed this value may deviate a little. The wide band gap of ZnO and TiO_2 (larger than 3 eV) is useful to avoid any parasitic light absorption and to prohibit the extraction of holes from the valence band of the perovskite. The electron mobility in ZnO is typically higher than TiO_2,[113,114] but since the thickness of the compact layer can be as low as 10 nm it is not clear if this difference can influence the cell's PCE.[108,115] Alternatively, SnO_2 is characterized by a higher electron mobility and larger bandgap than TiO_2 and ZnO and also is a UV stable material[116–118] whereas TiO_2 has shown to induce degradation in presence of UV-light.[39] ZnO was the first material implemented in flexible PSCs due to its easier low temperature processing with respect to TiO_2.[111] In the first report, a combination of electrodeposition of the compact layer and chemical bath growth of ZnO nanorods highlighted the versatility of ZnO in terms of low temperature deposition techniques that could be implemented, even if the PCE was limited to 2.6% on PET (8.6% on glass). The ZnO compact layer can be spin-coated from an ink dispersion based on ZnO nanoparticles, a procedure already extensively investigated in the field of OPVs.[119] This kind of ink was employed as the bottom layer in various reports on flexible PSC, but it can also be used as a top contact in inverted devices.[105,110,112,120] The same ink can also be deposited in glass/ITO/ZnO/perovskite/P3HT/Au structures by slot-die coating delivering a higher PCE of 10.3%. These nanoparticles were also used in an HTM-free flexible PSCs, in combination with a blade coated carbon paste, exhibiting a PCE of 4.3% and providing a first example of a fully printable flexible PSC.[110] To further improve the performance of ZnO based flexible PSCs, a ZnO layer was sputtered on a flexible glass-ITO substrate. In combination with an antireflective coating (see the complete stack in Fig. 1) the PCE of ZnO based devices was raised up to 13.1%.[101] It is also important to note that the highest PCE in f-PSCs till date is reported in a device employing ZnO ETL.[57] The PSCs employing a 40 nm ZnO compact layer on PEN-ITO, a ~380 nm thick $CH_3NH_3PbI_3$, and

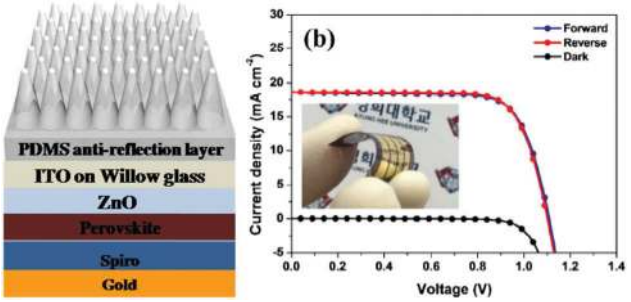

Fig. 1 Left, the stack of layers used for an ultrathin glass based flexible PSC. This configuration delivered an efficiency of 13.1%.[101] Adapted with permission from Highly Efficient Flexible Perovskite Solar Cells with Anti-reflection and Self-Cleaning Nanostructures, *ACS Nano*, **9–10**, 10287–10295.[101] Copyright 2015 American Chemical Society. Right, *J–V* curves of PEN/ITO/ZnO/$CH_3NH_3PbI_3$/PTAA/Au planar solar cell under 1 sun illumination (inset = photograph of corresponding flexible solar cell) delivering an efficiency of 15.4% (forward scan) and 15.6% (reverse scan) amongst the highest at the time of publication.[57] Reproduced from ref. 57 with permission from The Royal Society of Chemistry.

50 nm thick PTAA layer as HTM demonstrated PCE ~ 15.6% (see Fig. 1). The high PCE is attributed to the higher electron mobility in ZnO which also provided a balance of electron and hole flux within the device resulting in a hysteresis free PV performance (Table 1).

However, the use of ZnO might need some further optimization if one looks at the stability of the device. Indeed, especially when the ZnO is made at low temperature, it can rapidly induce degradation of the perovskite layer due to its basic nature.[121] This kind of interaction with the perovskite layer is even more evident when the formulation based on $PbCl_2$ is used. In this case the ZnO can strongly influence the perovskite growth, by making it faster and less efficient.[122]

A way to overcome these issues is to find an effective low temperature synthesis method for a TiO_2 compact layer. TiO_2 is widely used in n–i–p PSCs on glass where it is usually synthetized at high temperature. The most popular technique is spray pyrolysis, as a result of its easy processing and the high quality of the resulting films in terms of compactness and crystallinity.[123] The compact layer is often coupled with a mesoporous TiO_2 layer that improves collection of electrons and reduces hysteresis during IV measurement. However, both the compact and mesoporous TiO_2 are typically treated at high temperatures which are not compatible with polymer substrates. The compact layer has been often deposited *via* alternative techniques such as sputtering or atomic layer deposition (ALD). So far, only one study reports the use a mesoporous TiO_2 in flexible PSC on polymer films,[108] while it is more commonly used when the substrate is composed of a metal foil that can withstand higher temperatures.[124] In the former report, the same screen printable TiO_2 paste, conventionally sintered at 450–500 °C, underwent a UV-irradiation procedure[125] to remove the binders inducing a low temperature photocatalytical oxidation and improved particle necking.[108] The mesoporous TiO_2 was deposited over a ~11 nm amorphous ALD TiO_2 layer which showed good hole blocking behaviour owing to its compactness. Together with the fast charge injection in the

Table 1 Summary of different electron transport layers (ETL), perovskite synthesis, hole transport materials (HTM), top electrodes and their deposition technique, and the power conversion efficiencies (PCEs) of flexible PSCs in the n–i–p architecture fabricated on plastic/TCO substrates. The table specifies the coating technique, the synthesis approach, and the main lead salt used for the perovskite film. All the abbreviations not used in the text above are defined at the bottom of the table

Substrate	ETL	Perovskite synthesis	HTM	Top electrode	Notes	PCE [%]	Ref.
PEN-ITO	ZnO	Spin coating – 1 step – $MAPbI_3$	PTAA + Li-TFSI[b] + TBP[c]	Evaporated Au	High mobility ETL, ZnO	15.6	57
PET-ITO	Sputtered TiO_2	Spin coating – 2 step – $PbCl_2$	Spiro-OMeTAD + LiTFSI[b] + TBP[c]	Evaporated Au		15.1	99
PEN-ITO	$ZnSnO_4$ nanoparticles	Spin coating – 1 step – PbI_2 – solvent engineering	PTAA + LiTFSI[b] + TBP[c]	Evaporated Au		14.9	55
PET-ITO	e-beam TiO_2	Spin coating – 1 step – $PbCl_2$	PTAA + LiTFSI[b] + TBP[c]	Evaporated Au		13.5	100
Flexible glass – ITO	Sputtered ZnO	Evaporation – 2 step	Spiro-OMeTAD + LiTFSI[b] + TBP[c]	Evaporated Au	Antireflection coating	13.1	101
PET-ITO	None	Spin coating – 2 step – PbI_2	Spiro-OMeTAD + LiTFSI[b] + TBP[c]	Evaporated Au	Ultra-fast scan, no proof of steady state power production[98]	12.7	96
PET-IZO	100 nm TiO_2 nanoparticles (20 nm)	Spin coating – 1 step – PbI_2	Spiro-OMeTAD + LiTFSI[b] + TBP[c]	Evaporated Ag	Air assisted perovskite spin	13.2	102
PET-ITO	20 nm TiO_2 – atomic layer deposition	Spin coating – 1 step – $PbCl_2$	Spiro-OMeTAD + LiTFSI[b] + TBP[c]	Evaporated Ag		12.2	94
PET-ITO	ZnO sputtering	Evaporation – 2 step	Spiro-OMeTAD + LiTFSI[b] + TBP[c]	Evaporated Au	Inverted nanocone substrates	11.3	103
PEN-ITO	TiO_2 + PCBM	Spin coating – 1 step – PbI_2 – solvent engineering	PTAA + LiTFSI[b] + TBP[c]	Evaporated Au	Dripping with ethyl ether	11.1	104
PET-ITO	ZnO nanoparticles	Spin coating – 2 step – PbI_2	Spiro-OMeTAD + LiTFSI[b] + TBP[c]	Evaporated Ag		10.3	52
PET-ITO	FPI-PEIE/PCBM	Spin coating – 1 step – PbI_2 – solvent engineering	Spiro-OMeTAD + LiTFSI[b] + TBP[c]	Evaporated Ag		10.0	94
PET-ITO	Graphene + ZnO nanoparticles	Spin coating – 2 step – PbI_2	Spiro-OMeTAD + LiTFSI[b] + TBP[c]	Evaporated Ag		9.7	105
PET-ITO	60 nm TiO_2 – sol–gel	Spin or spray coating – 1 step – $PbCl_2$	Spiro-OMeTAD + LiTFSI[b] + TBP[c]	Evaporated Ag	Photonic sintering TiO_2	8.9	106
PET-ITO	100 nm metallic Ti – RF sputtering	Spin coating – 1 step – PbI_2	Spiro-OMeTAD + LiTFSI[b] + TBP[c]	Evaporated Ag		8.4	107
PET-ITO	11 nm TiO_2 – atomic layer deposition + 250 nm mesoporous TiO_2	Spin coating – 1 step – $PbCl_2$	Spiro-OMeTAD + LiTFSI[b] + TBP[c]	Evaporated Au	UV curing TiO_2 paste and series connected module	8.4	108
PET-ITO	ZnO + PCBM	Spin coating – 1 step – $PbCl_2$	P3HT[a]/dry PEDOT:PSS	Printed Ag		5.4	109
PET-ITO	ZnO nanoparticles	Spin coating – 2 step – PbI_2	None	Blade coated carbon paste		4.3	110
PET-ITO	50–200 nm ZnO (electrodeposition) + 400–500 nm ZnO nanorod (chemical bath)	Spin coating – 2 step dipping – PbI_2	Spiro-OMeTAD + LiTFSI[b] + TBP[c]	Evaporated Au		2.6	111
PET-ITO	ZnO nanoparticles slot-die coating	Slot-die coating – 2 step	P3HT[a] + LiTFSI[b] + TBP[c] (slot-die coating)	Evaporated Ag	Only module – No small area cell on PET – slot-die coating	1	112

[a] Poly(3-hexylthiophene-2,5-diyl). [b] Bis(trifluoromethane)sulfonimide lithium salt. [c] 4-*tert*-Butylpyridine.

overlaying mesoporous layer (250 nm thick) the flexible PSC delivered a PCE of 8.4%. The versatility and printability of such a TiO_2 paste allowed the fabrication of the first flexible perovskite module as will be detailed in the Section 10 of this article.[108] When the same ALD compact layer was employed in a planar PSC, limited charge injection resulted in a low PCE (~1%), higher hysteresis and lower stability. This means that the ALD process used in that study led to the fabrication of a good hole blocking layer with poor electron injection properties. The ALD process can, however, be tailored by changing precursors and processing conditions,[118] in order to even develop planar PSCs with PCE over 12%.[94] This highlights the importance of controlling the TiO_2 synthesis, since similar TiO_2 films can gives notably varying results.[24] Nevertheless, the exact requirements to obtain a compact TiO_2 layer suitable for planar PSC are still not clear, since both amorphous and crystalline compact TiO_2 may result in high efficiency as well as non-working devices.[126]

Even though crystalline TiO_2 can provide good charge extraction efficiency depending on the crystal phase and morphology used, to date one of the highest PCEs for flexible PSCs was obtained with an amorphous TiO_2 compact layer using a PET/ITO/TiO_2/perovskite/Spiro-OMeTAD/Au.[126,127] By optimizing the sputtering deposition of amorphous TiO_2 and employing a modified double step procedure for perovskite deposition (based on $PbCl_2$ and CH_3NH_3I vapour) the flexible PSC showed a remarkable PCE of 15.1% (see Fig. 2).[99] As explained in the paper, the oxygen vacancies present in the amorphous film led to a deeper Fermi level respect to the anatase counterpart, with beneficial effect on charge extraction.

Efficiencies of up to 13.5% were also obtained by employing an e-beam evaporated TiO_2 layer.[100] The importance of achieving pin-hole free compact layers was highlighted, since the presence of defects in them resulted in a non-homogenous defected perovskite layer over them. Another study proposed the use of a metallic sputtered Ti film (100 nm) with subsequent oxidation in air at high temperatures as a compact layer for flexible PSC providing not only effective extraction but also improved transmittance.[107]

Besides vacuum deposition techniques, TiO_2 compact layers have been successfully deposited in flexible PSCs *via* solution processing. Sol–gel synthesis is widely used in glass based devices, where it is possible to crystallize the deposited film by means of high temperature annealing.[32] Rapid photonic curing with infrared light (5 pulses of 2 ms with 19.3 J cm^{-2} radiant exposure) is one way to overcome this limitation on heat-sensitive substrates, and has been shown to lead to a massive improvement of the performance of the compact layer without damaging the plastic substrate (PCE increased from 1.8% to 8.1%).[106]

Photonic curing induces crystallization/annealing *in situ*, while an alternative strategy is to crystallize the ETL material prior to the deposition. Casting inks of TiO_2 nanoparticles mixed with sol–gel precursors (that act as a mortar between particles) has been an effective method to deposit crystalline TiO_2 layers at low temperatures. Glass based PSCs fabricated with this method yielded efficiencies of up to 19.3%.[91,128] Whilst on glass the size of TiO_2 nanoparticles used for the compact layer has usually been smaller than 10 nm in order to

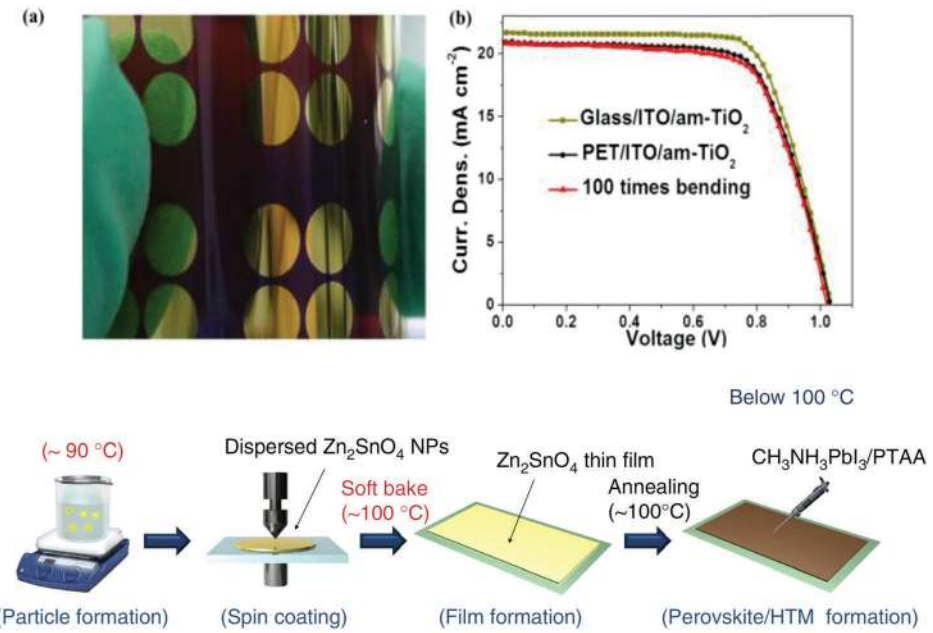

Fig. 2 Above: (a) Photograph of one of the best performing flexible PSC (PET/ITO/TiO_2/$CH_3NH_3PbI_{3-x}Cl_x$/spiro-OMeTAD/Au) reported at the time of publication with sputtered TiO_2 compact layer; (b) JV scan of the best devices on both glass and PET, showing also the curves after bending the latter for 100 times (radius of curvature not given).[99] Reproduced from ref. 99 with permission from The Royal Society of Chemistry. Below: Scheme of the low temperature synthesis and application of Zn_2SnO_4 nanoparticles for fabricating flexible PET/ITO/Zn_2SnO_4/$CH_3NH_3PbI_3$/PTAA/Au cells.[55] Adapted from High-performance flexible perovskite solar cells exploiting Zn_2SnO_4 prepared in solution below 100 °C, *Nat. Commun.*, **6**,[55] Copyright © 2015, Rights Managed by Nature Publishing Group.

obtain a more compact film, in flexible PSC, surprisingly, 20 nm sized TiO_2 nanoparticles were successfully employed without any additional precursor. In fact, even if it is not clear how such a potentially porous layer can prevent direct contact between TCO and perovskite, flexible PSCs with a PCE of 12.3% have been reported.[92]

The nanoparticle route has also been implemented with ternary oxide Zn_2SnO_4 nanoparticle dispersion synthetized at low temperature. Flexible PSCs with the Zn_2SnO_4 ETL achieved efficiencies of 14.7% as a result of the good hole blocking/electron injection behaviour and to the low refractive index of the ETL film (Fig. 2).[55] This latter feature reduces the reflections at the ITO interface, increasing light harvesting and the J_{SC} of the devices.

An attractive material that may be able to improve electron extraction from the perovskite and can strongly reduce the hysteresis effect is a well-known fullerene derivative, PCBM. PCBM is used in flexible PSCs in combination with another buffer layer, probably to mitigate the effect of the partial dissolution of PCBM in the perovskite solvent. In particular it was deposited on top of TiO_2 nanoparticles or on another fullerene derivative blended with an n-type polymer. In both cases the perovskite was synthetized with a solvent engineering method, and the PCE delivered by the cells were 11.1% and 10.3% respectively.[52,104]

6. p–i–n flexible perovskite solar cells with a bottom hole-extracting layer

In the p–i–n PSC structure, the TCO is coated with an HTM compact layer, and the perovskite is covered with an ETL above it. This architecture is generally similar to that of a polymer solar cell, benefiting from the know-how accrued on solution-processed HTMs and ETLs in the field of OPV. A summary of the results obtained on p–i–n flexible PSCs is shown in Table 2.

For this type of flexible PSC architecture, the HTM layer is typically deposited by spin coating PEDOT:PSS, a p-doped polymer, while PCBM is mainly used as the ETL. Both layers prove to be very effective in extracting charge and compatible with flexible PSC processing. Indeed with an evaporated Al top contact a 9.2% PCE can be obtained on PET-ITO with this very simple PET/ITO/PEDOT:PSS/perovskite/PCBM/Al structure (see Fig. 3).[120] Besides their suitable electronic properties (high work function for PEDOT:PSS[141] and high electron affinity and mobility for PCBM[142]), both layers are easy processable in solution and do not need high temperature treatment (*i.e.* <150 °C). PEDOT:PSS is deposited from a commercial water-based ink, with a thickness ~ 40 nm that ensures good hole extraction and high visible light transmittance.

Since the first report in PSCs, PEDOT:PSS has shown to offer a suitable material surface for perovskite growth, apart from its good hole-extracting capabilities.[95] Nevertheless, this layer is known to be unstable especially if ingress of water is not avoided by proper encapsulation. Therefore, despite the progress shown by flexible cells incorporating PEDOT:PSS, further understanding of its role in stability together with that of the perovskite layer (also susceptible to moisture ingress), is required as well as developing more robust substitute materials. In fact, a number of alternatives have been already demonstrated on glass substrates, leading to a strong enhancement of light-soaking stability, and a transfer of such alternatives to flexible substrate should be encouraged.[143] For the ETL layer, PCBM is typically cast from a chlorobenzene solution on top of the perovskite layer. So far, this material has been proven to be superior to TiO_2 in terms of its charge extraction properties.[144] When it is spin coated on top of the perovskite, PCBM is able to percolate along the grain boundaries, passivating the surface defects and providing a highly efficient PSC, usually with negligible or no hysteresis.[145]

Most research in p–i–n flexible PSCs has focused on the perovskite deposition and on the implementation of interlayers at the different interfaces. The perovskite film is usually cast with a 3 to 1 CH_3NH_3I:$PbCl_2$ solution, a formulation well suited for planar cells. Some further modifications have been proposed. For instance, an interesting development that further reduces the thermal budget in PSC fabrication is the use of NH_4Cl in the perovskite ink. It allows room temperature crystallization of the film yielding a PCE of 8.4% on flexible substrates.[136]

Deposition by evaporation of the lead salt or of the complete perovskite has been tested on flexible substrate. However, the PCE is still lower with respect to the state-of-the-art solution processed devices.[93,133] The best-performing cells were indeed obtained using the standard $PbCl_2$ formulation, with efficiencies of 12.5%.[132] In order to achieve such a high PCE, a top interlayer was employed. In addition to the standard PEDOT:PSS and PCBM (or PTCDI) layer, an additional Cr_2O/Cr double layer was evaporated between the ETL and the top gold electrode (Fig. 3, bottom). That interlayer prevented any reaction occurring between the top electrode and the perovskite layer, which would have otherwise led to device degradation due to interaction of the back contact (Ag) with the perovskite layer.

The top interface is investigated in several other reports, where a variety of materials were used to improve device performance. An additional interlayer can both fill the pinholes in the ETL layer and may act as an additional buffer layer to improve charge extraction. Indeed, it is not always possible to use PCBM on its own to get a working device, but it is unclear if this is due to the high roughness of the perovskite layer that needs to be covered further or to the electronic properties of the perovskite itself. Both organic and inorganic interlayers were implemented by using isopropanol as the solvent, since it does not dissolve the perovskite or PCBM. For instance a surfactant-modified C_{60} can be deposited on top of PCBM, as well as TiO_2.[95,135] The ETL may also be deposited by thermal evaporation. In that case, PCBM has proven to be superior to C_{60}, and an additional BCP hole blocking layer was added to C_{60} to further improve the structure.[140] Even the PEDOT:PSS surface can be modified to improve charge extraction. Additionally, this modification also influences growth of the perovskite, since it grows directly on the HTM.[146] For instance, a self-assembled monolayer of 3-aminopropanoic acid on PEDOT:PSS drastically changes the morphology of the film, leading to much smoother films with respect to pristine counterparts, leading to a 20% relative increase in the PCE.[139]

Table 2 Summary of different electron transport layers (ETL), perovskite synthesis, hole transport material (HTM), top electrode and processing techniques and the power conversion efficiencies (PCEs) of p–i–n flexible PSCs fabricated on plastic/TCO substrates. For the perovskite synthesis the coating technique, the synthetic approach and the main lead salt used are specified. All the abbreviations not used in the text above are defined at the bottom of the table

Substrate	HTM	Perovskite synthesis	ETL	Top electrode	Notes	PCE max [%]	Ref.
PET-ITO	NiO_x	Spin coating – 1 step – PbI_2 – solvent engineering	PCBM + BIS-C_{60}	Evaporated Ag	Surface nanostructured HTM – nanoparticles based ink	14.5	129
PET-ITO	PEDOT:PSS	Spin coating – 1 step – PbI_2 – solvent engineering	PCBM + LiF	Evaporated Ag	PEI-HI layered perovskite at PEDOT interface	13.8	130
PET-ITO	NiO_x	Spin coating	PCBM	Evaporated Ag		13.4	131
PET-ITO	PEDOT:PSS	Spin coating – 1 step – $PbCl_2$	PCBM	Evaporated Cr_2O_3/Cr/Au or Cu		12.5	132
PET-ITO	PEDOT:PSS	Evaporation – 2 step dipping – $PbCl_2$	PCBM	Evaporated Ca/Al	Layer by layer perovskite formation	12.3	133
PET-ITO	None	Spin coating – 1 step – PbI_2 – solvent engineering	PCBM	Evaporated Al	HTM free	9.7	134
PET-ITO	PEDOT:PSS	Spin coating – 1 step – PbI_2 – solvent engineering	PCBM + Bis-C_{60}	Evaporated Ag		9.4	135
PET-ITO	PEDOT:PSS	Spin coating – 1 step – $PbCl_2$	PCBM	Evaporated Al		9.2	120
PET-ITO	PEDOT:PSS	Spin coating – 1 step – $PbCl_2$ + NH_4Cl	PCBM	Evaporated Ca/Al	Non-thermal perovskite annealing	8.4	136
PET-ITO	PEDOT:PSS + PFI[b]	Spin coating – 2 step spinning – PbI_2	PCBM	Evaporated Al		8	137
PET-ITO	PEDOT:PSS	Blade coating – 1 step – $PbCl_2$	PCBM + Bis-C_{60}	Evaporated Ag	Blade coating of all active layers	7.5	138
PET-AZO-Ag-AZO	PEDOT + polyTPD[a]	Evaporated $CH_3NH_3PbI_3$	PCBM	Evaporated Au		7	93
PET-ITO	PEDOT	Spin coating – 1 step – $PbCl_2$	PCBM + TiO_2 sol–gel	Evaporated Al		6.4	95
PET-ITO	PEDOT:PSS + 3-aminopropanoic acid	Spin coating – 1 step – $PbCl_2$	PCBM-ZnO	Evaporated Ag	Roll coated HTM and perovskite	5.1	139
PET-ITO	PEDOT:PSS	Spin coating – 1 step – $PbCl_2$	PCBM-ZnO	Printed Ag paste	Roll coated active layer	4.9	109
PET-ITO	PEDOT:PSS	Spin coating – 1 step – PbI_2	PCBM + BCP	Evaporated Al	Evaporated ETL	4.5	140

[a] Poly[*N*,*N*′-bis(4-butylphenyl)-*N*,*N*′-bis(phenyl)benzidine]. [b] Tetrafluoroethylene-perfluoro-3,6-dioxa-4-methyl-7-octene-sulfonic acid.

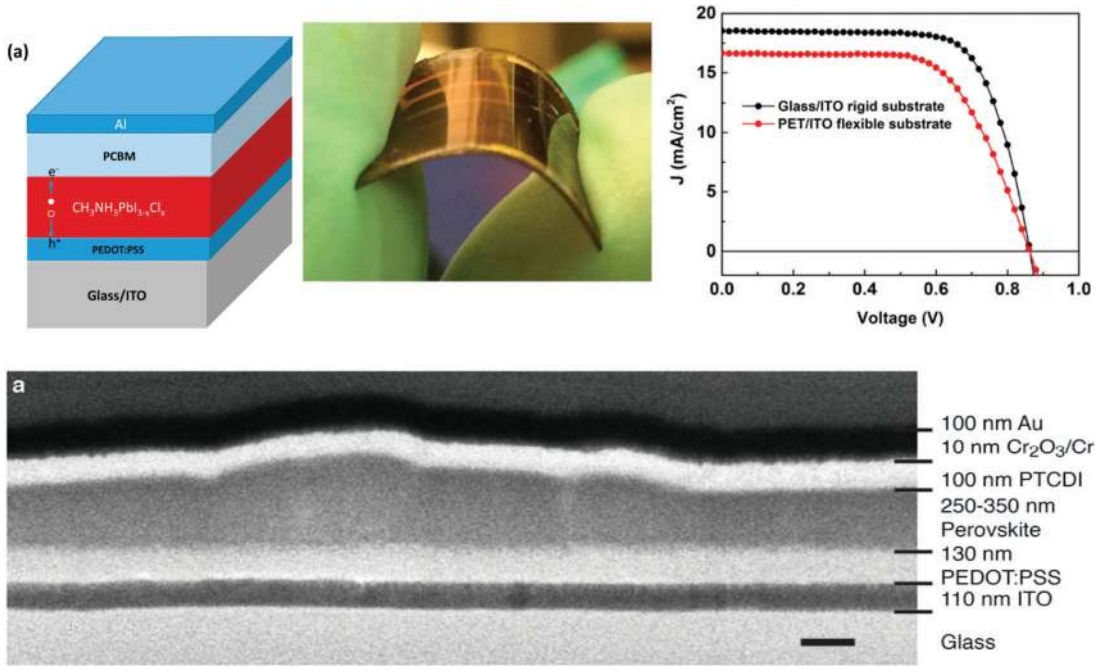

Fig. 3 Top: (left) The stack of layers used for a simple inverted flexible PSC (ITO/PEDOT:PSS/perovskite/PCBM/Al). (centre) A picture of the bent device on PET substrate and (right) is a comparison of the JV curves of the best PSC on glass and PET substrates.[120] Reprinted with permission from Low-Temperature Solution-Processed Perovskite Solar Cells with High Efficiency and Flexibility, *ACS Nano*, 2014, **8**, 1674–1680. Copyright 2014 American Chemical Society. Bottom: Cross sectional TEM (transmission electron microscopy) of the best performing p–i–n flexible PSC. The Cr_2O_3/Cr interlayer can be seen between the PTCDI and the gold.[132] Reprinted by permission from Macmillan Publishers Ltd: Flexible high power-per-weight perovskite solar cells with chromium oxide-metal contacts for improved stability in air, *Nat. Mater.*, **14**(10), 1032–1039. Copyright 2015.

Published on 09 September 2016.

The easier processing of such an architecture may allow faster upscaling with roll-to-roll compatible coating techniques. By using the know-how obtained in the OPV upscaling, two works on roll coating of flexible PSC have been published. The ETL is there composed of a PCBM–ZnO double layer, and both printed and evaporated silver were successfully employed on such a structure, leading to maximum PCE of 5.1% over 0.5 cm^2 of active areas.[109,139] However it is important to note that the planar device employing organic extraction layers (such as PEDOT:PSS and PCBM, for example) are suspected to degrade rapidly. This is due to the fact that both the layers are sensitive to humidity and PEDOT:PSS has an acidic nature that may corrode the substrate underneath.[140,147–151] Towards this end, alternative HTMs such as NiO_x have also been recently reported in f-PSCs by Zhang *et al.*[129] where a pin-hole free NiO_x ~20 nm layer in conjunction with $CH_3NH_3PbI_3$ and C_{60}/BIS-C_{60} resulted in PCE ~ 14.5% on PET-ITO substrates (~17.6% for ITO glass counterparts). The notable point here is that the NiO_x layer was deposited *via* spin coating without any further thermal or UV treatment and therefore the process is highly compatible with mass production.

7. TCO-free flexible perovskite solar cells

An interesting development of flexible PSCs is the demonstration of TCO-free devices. A summary of the results obtained on TCO-free flexible PSC is shown in Table 3.

At the beginning, the development of TCO-free PSCs served as a proof of concept of perovskite bendability.[88] Indeed a bending test on PET-ITO can only be conclusive until ITO does not crack, since the ITO layer is brittle and starts to fail before the perovskite itself, and the cracks propagate in the active layer leading to the device failure.[94] On the other hand, when a flexible bottom electrode is used instead of ITO, the PSC can be bent much more.[88] Since the main material used to substitute ITO is usually highly conductive PEDOT:PSS (even together with a conductive grid in the case of the most efficient TCO-free PSC), all the TCO-free PSCs published to date present a p–i–n structure. The only alternative to PEDOT:PSS tested to date are carbon nanotubes, but the PCE is limited to 5.4%.[155] Besides demonstrating the full range of flexibility of perovskite, the PEDOT:PSS-based devices also demonstrated ultra-lightweight capability. The best devices, with a PCE of 12%, were fabricated on a ultrathin 1.4 μm thick PET film (see Fig. 4 for the complete structure), leading to a record power per weight ratio of 23 W g^{-1} which is one order of magnitude larger with respect to conventional technologies (Fig. 4).[132]

Moreover, the device was extremely flexible and able to withstand several cycles of compression and re-stretching without being damaged. Another study also confirmed that PSCs can be stretched if the bottom electrode is designed carefully.[152] The very low weight and the stretchability of these devices pave the way to new applications, *e.g.* sourcing energy for solar powered flying drones.[156]

Table 3 Summary of different electron transport layer (ETL), perovskite synthesis, hole transport material (HTM), top electrode and processing techniques and the power conversion efficiencies (PCEs) of inverted flexible PSCs fabricated on TCO-free substrates. The perovskite synthesis the coating technique, the synthetic approach and the main lead salt used are specified. All the abbreviations not used in the text above are defined at the bottom of the table

Substrate	HTM	Perovskite synthesis	ETL	Top electrode	Notes	PCE max [%]	Ref.
PET (57 μm) with embedded AG mesh	PEDOT:PSS	Spin coating – 2 step spin coating – PbI_2	PCBM	Evaporated Al	Ultralight and highly flexible	14	56
PET (1.4 μm)	PEDOT:PSS	Spin coating – 1 step – $PbCl_2$	PCBM or PTCDI[b]	Evaporated Cr_2O_3/Cr/Au or Cu	Ultralight and highly flexible	12	132
Noland Optical Adhesive 63	PEDOT:PSS	Spin coating – 1 step – $PbCl_2$	PCBM	Eutectic Ga–In blend		10.8	152
PET	PEDOT:PSS + metasulphonic acid	Spin coating – 1 step – $PbCl_2$	PCBM/rhodhamine 101/ C_{60}/rhodhamine 101/ LiF	Evaporated Ag		8	153
PET	PEDOT:PSS	Spin coating – 2 step dipping – PbI_2	PCBM	Evaporated Al		7.6	154
PET	SWCNT[a]	Spin coating – 1 step – PbI_2 – solvent engineering	PCBM	Evaporated Al	HNO_3 doping of SWCNT[a]	5.4	155
PET	PEDOT:PSS	Spin coating – 2 step dipping – PbI_2	PCBM/TiO_2	Evaporated Al	Spray coating of PEDOT	4.9	88

[a] Single walled carbon nanotubes. [b] *N,N′*-Dimethyl-3,4,9,10-tetracarboxylic perylene diimide.

Fig. 4 (top) Device structure of the best performing TCO-free flexible PSC. (middle) Two photographs of the ultra-thin device before and after compression. No failure was observed after several compression cycles. (bottom) Comparison of power-per-weight ratio of different photovoltaic technologies relating to academic results of leading ultralight solar cells.[132] Adapted by permission from Macmillan Publishers Ltd: Flexible high power-per-weight perovskite solar cells with chromium oxide-metal contacts for improved stability in air, *Nat. Mater.*, **14**(10), 1032–1039. Copyright 2015.

8. Flexible perovskite solar cells on metal substrate

Metal foils are a valid alternative to polymer films. The advantages are their ability to withstand higher temperatures, higher permeation barrier properties and higher conductivity compared to conducting plastic substrates. The main drawback of using these substrates is the need to manufacture a transparent top electrode that has to be deposited on top of the perovskite layer stack without damaging it. A summary of the results obtained on metal-based flexible PSCs is shown in Table 4.

Unless one produces single cells and then connects them together, for practical industrial use, the metal foil is used only as a carrier, since it is hard to create the series connection of a

Table 4 Summary of different electron transport layer (ETL), perovskite synthesis, hole transport material (HTM), top electrode and processing techniques and the power conversion efficiencies (PCEs) of flexible PSCs fabricated on metal-based substrates. For the perovskite synthesis the coating technique, the synthetic approach and the main lead salt used are specified

Substrate	ETL	Perovskite synthesis	HTM	Top electrode	Note	PCE max [%]	Ref.
Titanium foil	TiO_2 nanowire array – hydrothermal synthesis	Infiltration – 1 step – PbI_2	Electrodeposited PEDOT	PEN-ITO	Top PEN-ITO-PEDOT clipped on Ti foil, perovskite ink infiltrated in the gap	13.1	157
Titanium foil	Compact TiO_2 spray pyrolysis + 300 nm mesoporous	Spin coating – 1 step – PbI_2 – solvent engineering	Spiro-OMeTAD + LiTFSI + TBP	Sputtered ITO (+ 1 nm evaporated Ag)	Electropolished Ti foil – $TiCl_4$ treatment	11.0	124
Titanium foil	50 nm compact TiO_2 sol–gel + mesoporous Al_2O_3	Spin coating – 1 step – $PbCl_2$	Spiro-OMeTAD + LiTFSI + TBP + V_2O_5 and PEDOT:PSS	Laminated PET/Ni mesh/adhesive PEDOT foil		10.3	158
Titanium foil	300 nm TiO_2 nanotubes – anodization + $TiCl_4$	Spin coating – 2 step dipping – PbI_2	Spiro-OMeTAD + LiTFSI + TBP	Transferred CNT	Spiro-OMeTAD deposited after CNT	8.3	159
Titanium foil	Spray pyrolysis + $TiCl_4$ + mesoporous TiO_2	Spin coating – 1 step – PbI_2 – solvent engineering	Spiro-OMeTAD + LiTFSI + TBP	Ag nanowires – spray coating		7.5	160
Titanium fiber (coil)	Anodized Ti	Electrodeposition – 2 step – $Pb(NO_3)_2$	Spiro-OMeTAD + LiTFSI + TBP	CNT	Elastic cells, also woven in textile	5.2	161
Titanium fiber	Anodized Ti + mesoporous TiO_2 dipping	Dip coating – 1 step – PbI_2 – solvent engineering	Spiro-OMeTAD + LiTFSI + TBP	Ag nanowires	Electropolished Ti foil – $TiCl_4$ treatment	3.9	162
Stainless steel Fiber	Dip coating ZnO seed + ZnO nanorod growth	Dip coating – 2 step – PbI_2	Spiro-OMeTAD + LiTFSI + TBP	CNT		3.8	163
Stainless steel Fiber	50 nm compact TiO_2 dip coating + mesoporous TiO_2 dip coating	Dip coating – 1 step – PbI_2	Spiro-OMeTAD + LiTFSI + TBP	CNT		3.2	164

monolithic module on a metal.[165] After depositing a planar insulator layer, the substrate is coated with a thin film electrode (usually metallic), easy to scribe with laser ablation. Without this process, mechanical cutting of the metal foil would be necessary to electrically isolate different areas, harming the mechanical stability of the foil. Mechanical cutting has been successfully employed in the industrial production of dye sensitized solar cells on titanium foil, because in that case a conductive foil (the counter-electrode) is laminated on the titanium foil, ensuring the mechanical stability of the device.[166] The same procedure might be applied to flexible PSCs, especially because a procedure to laminate a transparent and conductive top substrate has been recently demonstrated.[158] Nevertheless, the reports on flexible PSC on metal foil are currently limited to single cell development, thus the foil is used as the bottom electrode itself. In this case the roughness of metal foils can be an issue, and indeed the best performing devices implement an electropolishing pre-treatment on the metallic substrates.[124]

The reported metal based PSCs to date used a n–i–p architecture with a mesoporous layer, typically TiO_2. For this reason titanium foil is the most employed substrate. It naturally provides a native TiO_x layer and can be anodized to grow a layer of TiO_2 nanotubes on the surface.[159] A standard processing procedure based on of spray pyrolysis of compact TiO_2, spin coating of mesoporous TiO_2 and perovskite prepared with solvent engineering method (see right panel of Fig. 5), allowed the authors to obtain one of the most efficient devices of this kind with a PCE of 11.0%.[124] The top electrode was made by a well-established material, an Ag doped ITO layer. It was sputtered directly on top of the Spiro-OMeTAD, giving a good conductivity and a high transmittance.

Good results were also obtained with an Al_2O_3 scaffold layer. Beside the preparation of the ETL, perovskite and HTM layers,

Fig. 5 Top left, structure of a metal foil based PSC with a self-adhesive top electrode. Bottom left, a picture of the complete device.[158] Reproduced from ref. 158 with permission from The Royal Society of Chemistry. Top right, device architecture of the best performing PSC made on a metal foil. At bottom right, cross sectional SEM image of the same cell.[124] Reproduced from ref. 124 and 158 with permission from The Royal Society of Chemistry.

the most interesting aspect of this study was the lamination of a self-adhesive transparent electrode (see left panel of Fig. 5). This electrode was composed of a nickel mesh embedded in a PET foil, and covered with a pressure sensitive blend of PEDOT and an adhesive.[167] A simple lamination ensured good electrical contact and enabled to reach efficiencies of 10.3%.[158] The only concern may be in the use of PEDOT:PSS that may probably be replaced by more stable materials, such as carbon nanotubes or Ni nanostructures, unless high-performance flexible encapsulation is implemented.

Besides nanoparticle-based scaffolds, titanium foils can be anodized to grow a layer of TiO_2 nanotubes that can be used as a porous ETL. Such a layer was used to fabricate flexible PSC with a PCE of 8.3%.[159] Additionally, that cell employed a transferred CNT layer, another alternative to TCOs. Another TCO alternative is represented by silver nanowires which have been used to fabricated efficient semi-transparent rigid PSCs, but not yet in metal foil PSCs.[168] A top electrode made of silver nanowires has however been implemented in flexible PSCs based on metal fibers. In fact, a metal substrate can also be in the form of fibers or meshes, which have already been adopted in other PV technologies and OLEDs.[169,170] For these, it becomes impossible to employ standard coating techniques which require a flat substrate. The whole fabrication procedure is different from the one described so far for glass based or flexible substrates. Currently, a common coating technique is that of dip coating, since it allows one to coat uneven surfaces. The fiber can be made of stainless steel or titanium.[162,164] For the former, both TiO_2 and ZnO were tested as the ETL, with similar results (PCE $\sim$ 3%).[163,164] In addition to dip coating on metal fibers, chemical bath deposition or electrodeposition have also been employed. Electrodeposition has been proven to be a very effective method for the deposition of the lead salt for the double step synthesis, leading to a major increase of performance.[161] An effective way to coat the fiber with a transparent top contact is to wrap a CNT sheet around it, as shown in Fig. 6. The fabrication process becomes even more complicated when a coil-shaped fiber is used, with the purpose of fabricating a flexible and stretchable woven PSC.[161] In this case, two CNT sheets were used to contact the inner and the outer part of the coil.

Thanks to the use of a double step perovskite synthesis, the efficiencies were raised from 1% to 5%. A crucial step developed to achieve this result was the electrodeposition of $Pb(NO_3)_2$ that created a uniform seeding layer over the peculiar surface of the coil. These results demonstrate the versatility of perovskite synthesis and fabrication processes which are able to be adapted to a variety of different substrates.

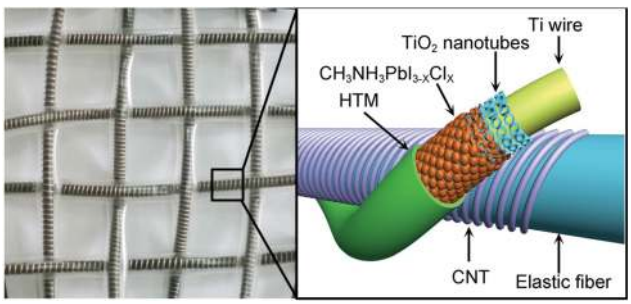

Fig. 6 Left, picture of a flexible PSC woven obtained with elastic Ti coil substrate. Right, a scheme of the device structure.[161] Reproduced from ref. 161 with permission from The Royal Society of Chemistry.

9. Upscaling from flexible perovskite solar cells to modules

Most of the reports published to date on flexible PSCs have been dedicated to small area cells, similar to their rigid counterparts. Nevertheless, there have been a handful of reports that investigate the upscaling of flexible PSCs. The upscaling from small area cells to large area module requires: (i) the development of large area coating techniques, (ii) patterned deposition or post-patterning procedures, and (iii) an optimized cell and interconnection design. Since the PSC module architecture resembles that of other thin film technologies, and requires optimization of cell dimensions,[43] a p1–p2–p3 laser scribing procedure is the preferred approach, since it enables the production of modules with very high aperture areas.[171,172] Nevertheless, in the early works on perovskite modules, patterning of the perovskite and HTM layers was carried out by manual removal on both rigid and flexible substrates (Table 5).[24,173–175] A first working small flexible module was demonstrated using the n–i–p mesoporous architecture. By combining laser patterning of masks for ITO, compact layer and gold, screen printing of the mesoporous layer and self-patterning of perovskite and HTM an efficiency of 3.1% was reached on a 5.6 $\times$ 5.6 cm^2 PET substrate (see Fig. 6), with the best cell of the module presenting a PCE of 4.3% (1.95 cm^2 active area).[108]

Whereas both ALD and screen printing are up-scalable techniques, spin coating is not. Thus, it is necessary to develop fully scalable processes for all layers for industrial purposes. Slot-die coating is very promising for this application, since it is compatible with the viscosity of the inks used for PSCs and deposits layers with the required thicknesses. Indeed, slot-die coating has been already investigated for both rigid and flexible PSCs.[112,176] On flexible substrates, the group at the Technical University of Denmark developed a R2R compatible process achieving a PCE of 4.9% (active area 0.2–0.5 cm^2) with all scalable techniques.[109] Indeed, one of the main advantages of developing PSCs on flexible substrate lies in its compatibility with R2R production. Another study also focused its attention on the slot-die coating and demonstrated a proof-of-concept of R2R fabricated flexible module (only the top electrode was evaporated), shown in Fig. 7. A double step process was instrumental to rapidly fabricate large area PSCs with a PCEs of roughly 1% over a substrate of 100 cm^2 providing an important proof of concept of upscalable R2R production.[112] The possibility of developing such a production process over large areas is an important aim of current research. In the next section we will delve into these possibilities further.

Table 5 Summary of different electron transport layers (ETL), perovskite synthesis, hole transport materials (HTM), top electrodes and their deposition technique, and the power conversion efficiencies (PCEs) of flexible perovskite solar modules. The table specifies the coating technique, the synthesis approach, and the main lead salt used for the perovskite film. All the abbreviations not used in the text above are defined at the bottom of the table

Substrate	ETL	Perovskite synthesis	HTM	Top electrode	Notes	PCE [%]	Ref.
PET-ITO	11 nm TiO_2 – atomic layer deposition + 250 nm mesoporous TiO_2	Spin coating – 1 step – $PbCl_2$	Spiro-OMeTAD + LiTFSI + TBP	Evaporated Au	4 cells – 8 cm^2	3.1	108
PET-ITO	ZnO nanoparticles slot-die coating	Slot-die coating – 2 step	P3HT + LiTFSI + TBP (slot-die coating)	Evaporated Ag	5 cells – 40 cm^2 – R2R coated	~1 (estimated)	112

10. Low temperature and roll-to-roll processing possibilities for f-PSCs

Processing of solar cells for new generation PV, including perovskites, can be divided into three categories as shown in Fig. 8; (i) single device fabrication, (ii) batch processing, and (iii) roll-to-roll (R2R, also called reel-to-reel) processing.[177,178] Single device fabrication is employed for laboratory scale cells (typically active areas ≤ 1 cm^2), both on rigid and flexible substrates, only for research and optimization purposes. The devices prepared by (ii) are usually modules, especially those on rigid glass substrates, which are significantly larger than laboratory scale devices (typically between 100 cm^2 and ≤ 1 m^2) and usually manufactured as a single unit or as a batch. (iii) R2R is instead a continuous web-based manufacturing process (at least till the substrates rolls are completely unrolled) and is employed for mass production of long flexible substrates (typically several tens of meters or even longer). The benefits of R2R in terms of processing and costs over large areas applied to the field of OPV have been reported by Krebs *et al.*[89]

So far, a number techniques compatible with mass production such as spray coating,[179,180] slot-die coating,[112,176] 3D or ink-jet printing,[181] and doctor blading[44,138] have been employed for fabrication of PSCs. Even if, at the moment, some of these studies have been applied to PSCs on glass only, they pave the way for being transferred to the manufacture of flexible PSCs, even for R2R processing. Barrows *et al.*[179] reported ultrasonic spray coating to develop planar heterojunction $CH3NH_3PbI_{3-x}Cl_x$ devices on pre-patterned ITO glass substrates with a perovskite surface coverage of over 80% by optimizing various processing parameters such as temperature of substrate, volatility of solvents and annealing conditions for perovksite film. They reported PCE ~11% in a champion device (area <1 cm^2) where only the perovksite film was developed using a R2R compatible method. The top and bottom polymer layers (PCBM and PEDOT:PSS, respectively) were deposited by spin coating which limited fabrication of a complete device using scalable methods.

Carbon based perovksite solar cells[68] employing an insulating scaffold layer and without a hole conductor are promising as their manufacturing is compatible with R2R processing. Wei *et al.*[181] developed, for the first time, carbon-based perovksite solar cells where the $CH_3NH_3PbI_3$/C bilayer is printed *via* an inkjet printer. They employed C/CH_3NH_3I ink formulation to chemically transform PbI_2 to $CH_3NH_3PbI_3$ *in situ* and reported PCE ~ 11.6% in their laboratory scale glass based PSCs. Recently, a modified 3D printer has also been employed for large area printing of PSCs. Vak *et al.*[176] reported 3D printer assisted slot-die coating to solution process various materials components of PSCs and obtained PCE ~ 11.6% for laboratory scale devices and ~4.6% for modules built on large area ITO glass substrates (~48 cm^2). To further improve the perovksite film quality using slot-die, gas-quenching assisted slot-die coating was introduced with PCE ~ 12% in fully printed PSCs (area <1 cm^2) on ITO coated glass substrates.[176] The ETL, perovksite as well as HTM layers were printed using slot-die whereas the top contact was deposited in vacuum. Similarly, a

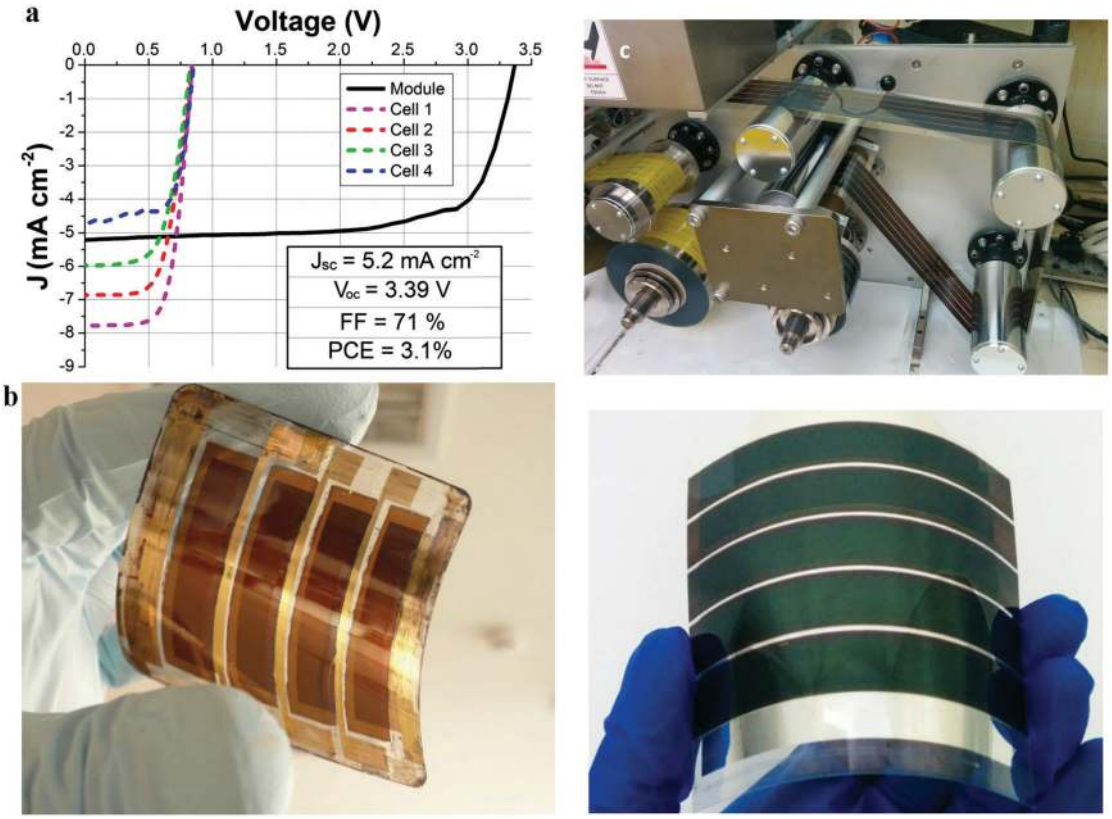

Fig. 7 (a) JV curves of a flexible series connected mini-module, together with the JV scans of the four constituent cells, (b) photograph of the mini-module whose JV curves are shown in (a).[108] Reproduced with permission form *Adv. Energy Mater.*, 2015 Wiley. (c) Photograph of the roll-to-roll double step production of a perovskite layer, showing the conversion from lead iodide (yellow) to perovskite (dark brown).[112] (bottom) picture of the completed roll-to-roll flexible PSC module with an evaporated Ag contact.[112] Reproduced with permission form *Adv. Mater.*, 2015 Wiley.

recent report by Yang *et al.*[182] has also shown fully printable PSCs on glass ubstrates by doctor blading. Although these processes were developed on rigid substrates the devices are processed at low temperature (except annealing of ETL where required); and therefore, they can be extended to flexible substrates. On the other hand, vacuum processing of the perovksite layer[183,184] has also demonstrated its compatibility with batch processing, however limited to rigid substrates so far. Batch processing of flexible large area PSC module by screen printing and UV-assisted processing was first established by Di Giacomo *et al.*[108] with PCE $\sim$ 3.1%.

Schmidt *et al.*[109] developed the first fully printed flexible PSCs *via* R2R compatible methods on ITO-polyethyleneterphthalate (PET) and reported PCE $\sim$ 4.9%. This was around half the PCE value of cells manufactured via spin coating on ITO/glass substrates, a similar trend to that observed in printed OPV. Similarly, Das *et al.*[106] showed combined ultrasonic spray-coating and photonic curing to process flexible PSCs (PCE 8.1%) on PET, a method that can be applied to R2R processing and also can yield pin-hole free high quality perovksite layers. In all reported methods, perovksite annealing typically takes 45–60 min which may hinder R2R processing. To overcome this issue, Troughton *et al.*[185] introduced rapid near infrared processing of perovksite precursor which only require 2.5 s with no notable decrease in cell performance. More recently the same group brought the value down to the ms range *via* photonic curing.[186]

Based on these developments one can conceive a promising future for R2R processed large area PSC modules. Fig. 8 shows manufacturing techniques that have been already successfully used in PSCs and/or OPV or DSCs such as laser processing,[172] flexographic printing, slot-die coating and rotary screen printing,[177,187,188] screen printing,[89] and gravure printing.[189] Some of the printing, coating and processing techniques not employed in PSCs so far but in the other two technologies can be investigated for the manufacturing of flexible PSCs in the future.[18,89]

11. Stability of flexible perovskite solar cells

When it comes to practical deployment, stable performance over time of a PV technology becomes as important as efficiency.[190] Despite the high efficiencies reported in PSCs, there have been concerns over their long term operational stability. Their performance is not only known to degrade over time due to intrinsic reasons such as structural instability[191] and their interaction with the selective transport layers,[192,193] but also, due to extrinsic factors such as moisture,[41,194]

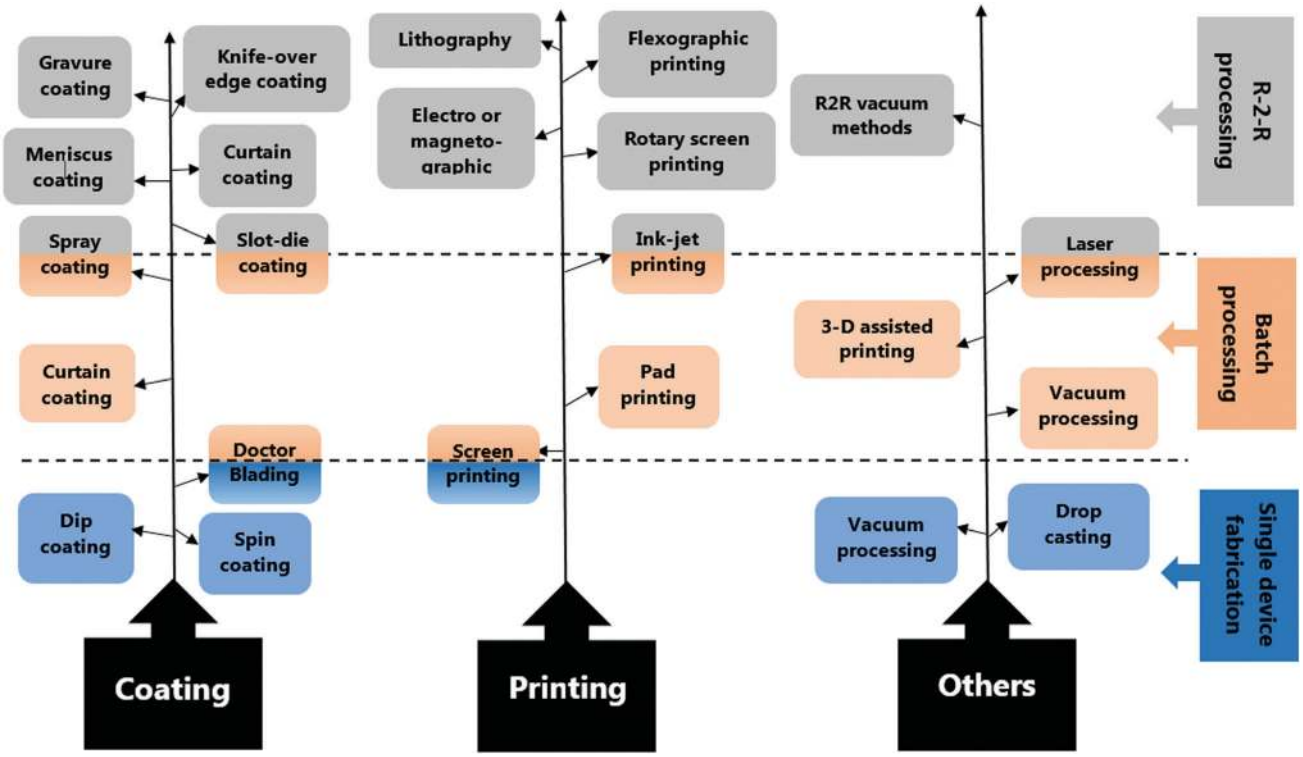

Fig. 8 Commonly employed device fabrication techniques for future generation solar cell such as organic solar cells, dye-sensitized solar cells and for the more recent perovksite solar cells. The fabrication techniques are classified vertically as coating, printing and others and horizontally based on its typical use, *i.e.*, laboratory, batch or R2R scales. A dual colored entry on the line means that the technique fills the requirements for both categories above and below it.

UV-light,[39] photon dose,[195] temperature[196] and hysteresis due to light soaking,[197,198] temperature[40] and their slow charge dynamics.[199,200] Flexible PSCs are even more sensitive to these factors as they are more difficult to be encapsulated effectively. They are manufactured on polymer substrates such as PET or PEN which are much more permeable to ingress of moisture and oxygen compared to glass counterparts and are possibly more prone to effects of high temperature cycling and UV exposure which a PV device typically faces when installed outdoors. Thus, stability must be ensured *via* a twofold strategy: the development of more stable perovskite, ETLs, HTMs and contact material combinations as well as effective permeation barriers (also used for flexible OPV[201] and DSCs[202]) and sealing of cells to minimize the effect of external factors.

The first systematic stability investigation of a f-PSC was reported by Weerasinghe *et al.*[102] who employed PET films coated with indium-doped zinc oxide substrates, with mesoporous TiO_2 as an ETL subsequently coated with $CH_3NH_3PbI_3$ and Spiro-O-MeTAD whereas an evaporated Au layer was used as top contact. The devices were encapsulated in a N_2 filled glove box using $\sim$85 μm thick plastic sealant (Viewbarrier, Mitsubishi Plastic, Inc., Fig. 9a) with water vapor transmission rate (WVTR) of 5×10^{-3} g m^{-2} day^{-1}. Three types of devices (encapsulated, partially encapsulated and un-encapsulated) were stored at ambient conditions ($T < 25$ °C, Rel. H 30–80%) and a shelf-life test was carried out for 500 h. The bare PSCs failed after just 100 h whereas the partially and fully encapsulated devices showed relatively slower degradation over time and retained at least $\sim$80% of initial PCE after $\sim$400 h (Fig. 9b). One of the main causes of degradation is moisture and oxygen ingress, especially through the adhesive layers and edges and around the wire contacts and results suggesting that the loss of device performance is associated with the formation of more resistive interfaces within the device.

Similar to glass based PSCs, it is not only the encapsulation that is required to achieve long term stability but also the right intrinsic material combinations. For example, the presence of a scaffold has been shown to lead to longer shelf lives in n–i–p PSC not only in glass based devices,[192,193] but also in plastic cells. In fact, after keeping the un-encapsulated devices in a dry box for a week, a scaffold-less cell lost 84% of its initial PCE while the cell incorporating a scaffold lost only 8%.[108]

A paper reporting one of the highest efficiencies for f-PSCs (PCE $\sim$ 14%), also investigated the mechanical and thermal stability of their ultrathin cells.[56] The substrate ($\sim$57 μm) consisted of an Ag-mesh (thickness $\sim$2 μm) embedded in a PET film subsequently coated with a high-conductivity transparent conducting polymer (Clevios PH1000). The bottom of this modified PET substrate was laminated on a $\sim$100 μm thick highly hardened PET to provide mechanical robustness. The PSCs built on these substrates (sheet resistance as low as $\sim$3 Ω sq^{-1} and high transmittance of $\sim$85%) showed remarkable mechanical stability after 500 bending cycles. The PSCs also retained >90% of their initial PCE after 500 h of storage at

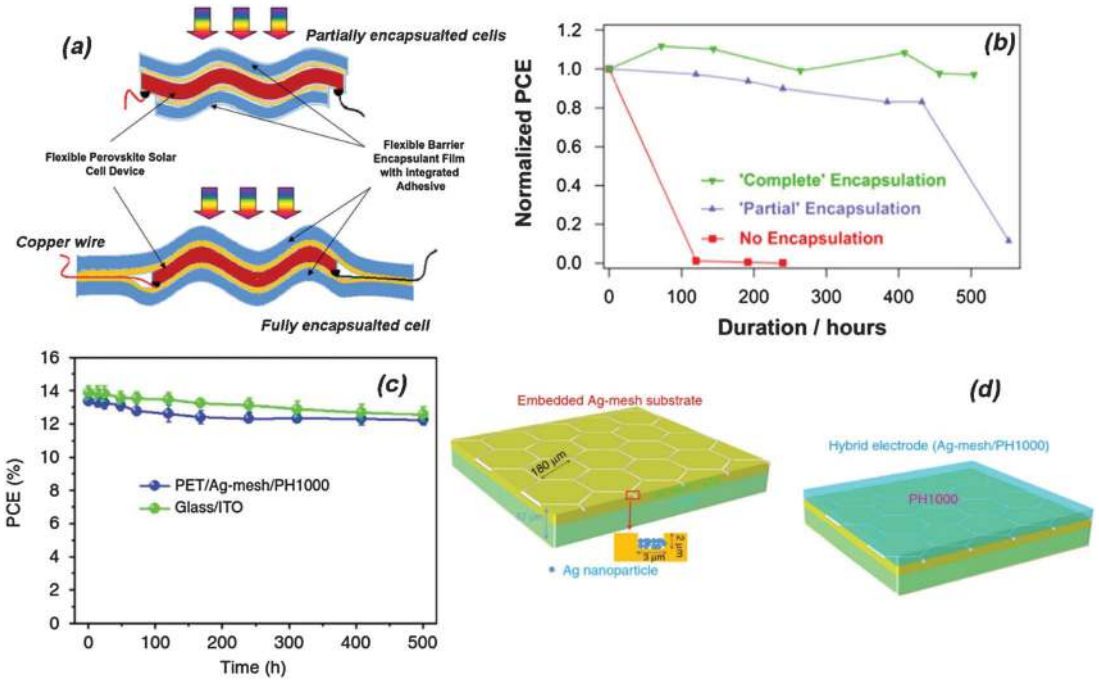

Fig. 9 (a) Schematic diagram showing (top) 'partial' and (bottom) 'fully' encapsulated flexible PSC architectures, (b) normalized PCE of non-encapsulated, 'partially'-encapsulated, and 'completely' encapsulated F-PSCs as a function of storage time under ambient conditions. Reproduced with permission from ref. 102, copyright of Elsevier, and (c) PCEs aging of f-PSCs fabricated on both PET/Ag-mesh/PH1000 and glass/ITO substrates at room temperature in N_2-filled glove box, and (d) schematic illustration of the hybrid electrode (PET/Ag-mesh/PH1000) (left) and (right) Ag-mesh, PET/Ag-mesh/PH1000-based substrates. Reproduced with permission from ref. 56, adapted by permission from Macmillan Publishers Ltd: *Nat. Commun.*.

room temperature in N_2-filled glove box. Stability testing of f-PSCs at 45 °C after 500 h and 70 °C after 100 h of storage showed ~25% and ~80% drop in PCE respectively, similar to that of a control device built on ITO glass thereby evidencing that the substrate does not lead to additional instabilities under these temperature tests, although these cells were kept in inert environment thus eliminating the effect of ambient water vapor and oxygen. To evaluate stability of f-PSCs in presence of humidity and at indoor conditions, Kaltenbrunner *et al.*[132] reported promising air-stability in ultrathin (~3 μm) f-PSC (PCE ~12%, power-per-weight as high as 23 W g^{-1}). The improved air-stability was obtained introducing (i) a chromium oxide–chromium (Cr_2O_3/Cr) interlayer between metal contact and perovskite to avoid possible reaction between the two, and (ii) polyurethane protective layer on top of the metal contact (Fig. 3).

The stability results show that similarly to other PV technologies such as OPV and DSCs developed on plastics, their long term stability will require effective encapsulation prior to air exposure. This can be implemented *via* plastic or multilayer barriers having adequate WVTRs[18] such as those developed for OPV. Furthermore, as PSCs are known to degrade under UV light, although it is known to effect more the TiO_2 based PSCs (PSCs built by replacing TiO_2 with Al_2O_3 suppressed UV-degradation),[39] UV light has to be shielded both from the internal layers and from the substrate if PEN is utilized. This would require additional UV-filters or UV-filtering substrates for f-PSCs if they are to be placed for outdoors. Note that f-PSCs could offer many advantages of being able to be integrated in objects for indoor applications since PSCs (on glass substrates) have recently shown to work efficiently under low light levels.[203] This could lower stability constraints on f-PSCs as they might not need to be exposed to high temperatures and UV-light as in the case of device built for outdoor applications. Research need to be carried out to understand the interaction of perovskite with PET and PEN, and their TCO-coated counterparts, a common issue observed in flexible DSCs where liquid electrolyte degraded ITO surface over time.[18] As can be noted from this section, the literature focusing on the stability of f-PSCs is much less broad compared to that focusing on efficiency and more work needs to be carried out in this field.

12. Cost and lifecycle analysis of PSCs

12.1. Markets and cost analysis of PSCs (cost per W_P, LCOE and balance-of-systems cost)

A solar cell technology wanting to penetrate the market should offer four key features, *i.e.*, high efficiency, low cost, long term stability, and added functionality (flexibility, transparency, easy integration and aesthetics *etc.*).[7] Silicon solar cells, although providing long lifetimes (~20 years) and high efficiencies (typically >20–25%), are relatively expensive (although costs have gone down significantly in the last 5 years), rigid, opaque and bulky. New generation solar cells such as OPV and DSCs currently suffer from relatively lower efficiency (typically ~10–13%) and

Table 6 Estimates for costs of perovskite solar modules. Values are taken from ref. 205 if not stated otherwise. The values in the table are those for the best case low estimates

	Glass substrates		Flexible substrates		Metallic substrates	
Description	Research scale $ per m^2	Cost MW ($ per m^2)	Research scale $ per m^2	Cost MW ($ per m^2)	Research scale $ per m^2	Cost MW ($ per m^2)
Substrates	14	10	9[a]	6[b]	2[c]	1
TiO_2 layer	0.2	0.06	0.2	0.06	0.2	0.06
Perovskite	1.33	0.44	1.33	0.44	1.33	0.44
HTM	1.5	0.49	1.5	0.49	1.5	0.49
Back contact	1.5	0.49	1.5	0.49	1.5	0.49
Solvents	8.9	2.95	8.9	2.95	8.9	2.95
Sealants	3[d]	2.5[b]	4[d]	3.25[b]	4.5[e]	3.75[b]
Encapsulating materials	5[d]	4	0.5[e]	0.05	0.5[e]	0.05
Electrical interconnections	N/A	2.9[206]	N/A	2.9[54]	N/A	2.9[206]
Total material cost		**23.83**		**16.14**		**12.13**
Capital investment	N/A	3.33[f]		2.47[f,g]		3.3[f]
Overhead cost		13.8[206]		10.3[g]		13.8
Labor cost		6[206]		4.6[g]		6
Total manufacturing cost		46.49		**34.28**		**35.23**
Cell yield 90%						
Manufacturing cost for cell yield		51.13[h]		37.71[h]		38.75[h]
Module cost in $ per W_P (PCE ~5%)		1.02[i]		0.75[i]		0.77[i]
Module cost in $ per W_P (PCE 10%)		0.51[i]		0.38[i]		0.39[i]
Module cost in $ per W_P (PCE 15%)		0.34[i]		0.25[i]		0.26[i]

[a] Cost of flexible substrates (PET/PEN) is ~30% lower than conducting glass substrates (ref. 54). [b] Cost reduction factor from ref. 205 is used when transforming research scale to MWs. [c] Cost of metallic substrates (Ti/Al) is ~90% lower than conducting glass substrates (ref. 54). [d] Ref. 206 and ref. 54. [e] Price is taken from Alibaba for plastic rolls for lamination and encapsulation.[204] [f] Taken from ref. 54 and 206 and a report of 20 MW production of dye-sensitized solar cells (ref. 207). As the number of steps involved in organic solar cells and PSCs are similar and also almost all manufacturing equipment, we assume similar capital investment for both. [g] Preparation of flexible devices avoids twice sintering of electron transport and hole blocking layers and thereby avoids two steps out of total eight steps required for a typical glass based PSC (substrates preparation, printing of hole blocking layer, m-TiO_2 layer and subsequent sintering, deposition of perovskite, HTM, evaporation of back contact, electrical connections, sealing and packaging). We therefore used a factor $6/8 \times (x)$ for the calculation of overhead cost and labor in case of flexible devices. [h] $46.49 \times 1.1 = 51.13$. [i] (51.13$)/(1000 $W_P \times$ efficiency). The formula is adopted from ref. 206.

shorter lifetimes although providing added interesting functionalities (*e.g.* transparency, flexibility, indoor performance) and low cost fabrication. PSCs may be able to provide many of these features simultaneously: not only has it shown to deliver a comparable PCE ~ 21% to silicon but can also be printed on flexible substrates and even made semi-transparent. These features make PSCs very attractive for commercial deployment. There still remain, however, concerns over its stability as described in the previous section.

A realistic figure for industrial costs for PSCs is hard to estimate at present with no installed facility for large scale manufacturing. However, as the PSCs device architecture and fabrication processes are similar to those of the DSCs and OPVs, particularly those made on flexible substrates and employing a scaffold layer, the costs associated to most of the materials and manufacturing processes of PSCs are conceivably similar. Unlike OPVs and DSCs, PSCs can be made in many different architectures (mesoporous, planar, meso-superstructured, HTM free, ETL free *etc.*) and with at least four perovskite synthesis techniques (single step, double step, dual source evaporation and temperature assisted vacuum evaporation). In Table 6 we present an estimated cost analysis using the most commonly employed device architecture, *i.e.*, employing a TiO_2 scaffold layer and also widely adopted fabrication methods of solution processing (single or double step fabrication). The reason of this selection is twofold: the device architecture and the methods have delivered PCE >15% (on glass) by numerous groups worldwide and certified efficiencies are also reported using these two architectures (mesoporous and planar). The cost of a photovoltaic technology is usually given in $ per W_P, which includes the manufacturing cost of solar modules (materials, processing and capital investment) and is a parameter usually used to compare cost of various types of solar modules. Table 6 lists cost breakdown of materials, manufacturing processes, labor, capital investments, and other overhead cost for flexible *vs.* rigid PSCs according to the references.[54,204–207] The cost of electrical support system and site preparation is typically equal to module cost per W_P of PVs (1 : 1).[208] A major share (40–50%) of the total manufacturing cost of PSCs arises from their passive components (sealants, packaging and electrical interconnections). As the sealing of flexible devices requires more precision, the sealant cost for these (3.25–3.75$ per m^2) is anticipated to be higher than that of their glass based counterparts (2.75$ per m^2).[54,206] In fact, this estimation assumes a relatively simple encapsulation but if more complex multi-layer ultra-high permeation barriers are required then these can increase significantly (although they should be kept below 15–20% of total device cost). Among the active materials, substrates contribute the most to the manufacturing cost, *i.e.*, ~40%, ~36% and ~8% for ITO coated glass, PET/PEN and metallic substrates,

respectively and future cost reduction largely depends on the reduction of substrates price. A reduction in labor cost is also anticipated for flexible PSCs on PET/PEN as they can be made *via* roll-to-roll processing at low temperature and avoid dual sintering process at higher temperature $\sim$450 °C for compact and mesoporous layer which is employed for glass based counterparts.

It is also interesting to estimate the levelized cost of energy (LCOE) which includes both cost per W_P and balance of system cost (BOS, solar panel installation, framing and electrical supporting units such as invertors, wiring, storage if the PV installation is off-grid, maintenance, and licensing *etc.*) and can be simply expressed as, LCOE = Sum of cost over PV lifetime/sum of electricity produced over lifetime.[13] While cost per W_P is based on the maximum achievable output of PV installation, LCOE provides information based on the actual attainable power during a certain time (capacity factor) making it a more reliable measure for comparison.[208] To achieve a lower LCOE of PVs to match grid parity ($<$\$0.05 kW h),[13] not only the cost per W_P should be reduced but also, more importantly, the high efficiency of the modules over device lifetime should also remain stable (*i.e.* lifetime is very important). It is noteworthy that f-PSCs may offer additional cost-reduction during installation as they may not require intensive framing and mechanical support; however, the lifetime of $>$20 years will remain a challenging task. Although it is hard to calculate the LCOE of the PSCs at the moment as no commercial deployment is reported so far, a general understanding (for any PV technology) is that, if the total cost is lower than 1\$ per W_P (0.5\$ for module and 0.5\$ for installation) and assuming anticipated lifetimes $>$20 years, the LCOE can reach $\sim$0.5\$ kW h to meet grid parity (assuming high illumination conditions).[13] The manufacturing cost of flexible PSCs can be estimated to go well below 0.5\$ per W_P (0.4–0.25\$ per W_P) considering 10–15% efficient devices, (Table 6); however, concerns overs their shorter lifetime should be addressed in order to achieve low LCOE targets and the efficiencies at the large-area module scale need also significant improvements. The installation cost will also depend on price of electrical support system and energy storage system (in case of off-grid applications).[208] Flexible PSC modules although providing lower PCEs compared to glass based counterparts, can potentially entail lower installation costs as they can be integrated as BIPVs and other integrated applications easily. However, a key challenge is their stable performance over time as LCOE strongly depends on the device lifetime, *i.e.*, decreases with increasing device lifetime. Apart from consideration on cost \$ per W_P we have outlined above, it is worth noting that it is likely that PSCs in their flexible form will initially find their way into powering electronic products[18,82,209,210] indoors/outdoors (high estimated efficiencies, of up to $\sim$23–27% on glass-based devices, have been recently obtained under indoor artificial lighting in planar,[211] mesoscopic[212] and even flexible[213] perovskite cells) rather than (or as well as) large scale deployment outdoors so that cost considerations need to be applied and tailored for these different applications.

12.2. Life cycle analysis

The two main issues that have been discussed as potential roadblocks to a near future deployment of PSCs, despite the rapid progress made, are their operational stability and the content of lead even if it is rather minuscule per m^2. The most successful PSCs so far are made of $CH_3NH_3PbX_3$ (where X = Cl, I, Br) or with mixed formamidinium-methylammonium cations. It thus becomes important to investigate the potential risks associated to the health and environment related to Pb content.[214,215] There has been much discussion about replacing Pb with other elements such as Sn to overcome the potential toxicity and environmental impacts. However whereas efficiencies above 20% have been reported for $CH_3NH_3PbX_3$ based cells, those incorporating tin instead of lead have achieved a maximum PCE of 6.4%[216] with significant question marks over stability. A recent life-cycle analysis of lead and tin based PSCs by Serrano-Lujan *et al.*[214] discerns many disadvantages related to the latter. Not only the fact that tin metal is 6.3 times more expensive than lead, but, from the life-cycle perspective, the environmental impacts caused by tin based PSCs (accounting material extraction and device fabrication) produced on a functional scale (1 kW h) were estimated to be nearly double to that of lead based PSCs. This is due to the fact that the PCE of former is only one-third of the latter and it requires 3 times larger areas to produce 1 kW h of energy. This leads to higher resource utilization for tin-based PSCs and thereby 9.4 kg kW^{-1} h^{-1} CO_2 emission, almost double than that for lead based PSCs. Assuming conservatively a 10% efficient commercial f-PSCs module then it would require $\sim$80 cm^2 to produce 1 kW h compared to $\sim$48 cm^2 for a 15% efficient glass based counterpart (at 1 sun conditions). Thus, it becomes clear that to fully utilize the potential advantages relating to environmental impacts of both tin based PSCs and f-PSCs one needs to further improve their PCE and stability.

The environmental impacts (EI) of PV technology can be classified in three categories: (i) toxicity (cancer, non-cancer and human health), (ii) fresh water contamination, and (iii) resource depletion.[215] These include not only material extraction, resource utilization during manufacturing of PVs and the impact during lifetime but also the life-cycle during or after disposal *via* landfill or incineration. In term of resource depletion, f-PSCs offer advantages over glass based counterparts reducing EI by $\sim$40% (mainly by reduction in energy required for ETL annealing and FTO/ITO substrates heating/cleaning)[214] and also during re-cycling, thus reducing CO_2 footprint. However, the f-PSCs, if land-filled, are reported to have 5 times higher impact (human toxicity, fresh water and marine eutrophication) than if incinerated,[214] primarily due to presence of lead. On the other hand, if incinerated, the environmental impacts caused by PET alone are estimated to cover a large percentage of fresh water ecotoxicity (97%) and of human toxicity (noncancer effects). Also important to note that the economic benefits from lead recovery are almost negligible as in a typical device, lead accounts for $\sim$0.55% of total material,[214] although the amount is slightly higher than the allowed limit set by European restriction on hazardous substances.[217] This demands for efficient

strategies not only during manufacturing process to yield highly efficient flexible devices but also more efficient ways for their recycling and encapsulation during lifetime so as to avoid their potential surplus risks. More research needs to be carried out in this arena as well as liaising with appropriate institutions and stakeholders.

13. A perspective on publications and patents covering flexible perovskite solar cells

The PCE of PSCs has increased dramatically since 2009 owing to a remarkable growth in research activities worldwide as

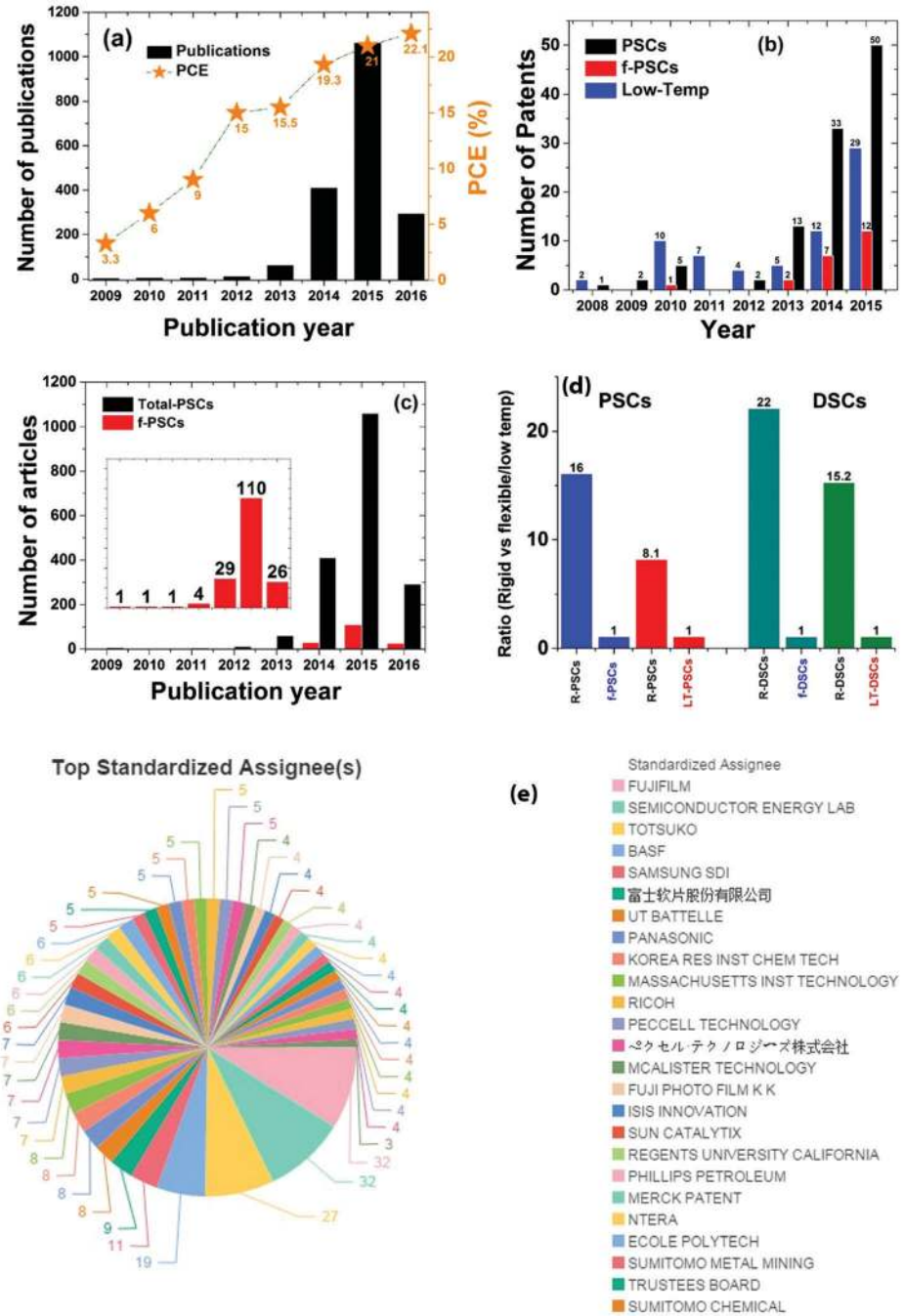

Fig. 10 (a) Number of publications on perovskite solar cells (bar graph) and their maximum power conversion efficiency (PCE, represented by the star symbol), (b) number of patents published on three types of PSCs (flexible, low temperature and on rigid substrates) over past 6 years, and (c) statistical comparative analysis of research publications for flexible *vs.* all perovskite solar cells published between 2009 and 15 March 2016. Publication data taken from Scopus. (d) The figure is drawn from data taken from Scopus database (30 October 2015) and presents a statistical analysis of publication in PSCs and DSCs (rigid substrates (R) *vs.* flexible (f) and high temperature *vs.* low temperature (LT)), and (f) Top assignees for rigid or glass based PSCs. Top assignees for f-PSCs and LT-PSCs are given in ESI† (Fig. S7).

witness the number of papers published each year in the field (see Fig. 10a). At the same time, industrial efforts to transform PSCs from a laboratory technology to one ready for commercial deployment have also led to a growing number of patents published (see Fig. 10b). The rising bar charts show how much interest is being focused both academically and industrially in this field.

13.1. Patent trends in PSCs and f-PSCs

We carried out a patent search employing 'Patsnap', a database that gathers intellectual property information from various major patent organizations such as the European Patent Office (EPO) and the World Intellectual Property Organization (WIPO). Although, the keywords used, *i.e.*, ''perovskite solar cells (PSCs)'', ''low temperature perovskite solar cells (LT-PSCs)'' and ''flexible perovskite solar cells (f-PSCs)'' revealed ~721 hits for 'PSCs', 580 for 'LT-PSCs' and over 100 for f-PSCs a precise screening of the patent list narrowed the numbers to 108, 69 and 22, respectively. The 'LT-PSCs' includes devices made on rigid conducting substrates (ITO or FTO) using low temperature processing ($T < 150$ °C) and thereby can also potentially be transferred to conducing plastic substrates. Unlike DSCs, where the ratio of patent hits for flexible/low temperature *vs.* rigid is very low (1 : 21), statistics in Fig. 10(d) show that this ratio for PSCs is significantly higher (1 : 15). It is likely that this strong industrial interest is primarily due to the fact that 'LT-PSCs' and 'f-PSCs' have delivered high PCEs of ~15% and ~15.6%[57] at standard test conditions, respectively, (significantly higher compared to DSCs and OPV counterparts) thereby offering strong appeal for industrial competitiveness at the efficiency level. The patents statistics also reveal notable commercial interests worldwide as a great number of patents in all three categories (PSCs, 'f-PSCs', and 'LT-PSCs') have been published by the industrial sector from Europe, United States and Asia (Fig. 10e and Fig. S7, ESI†).

Among the patents filed on f-PSCs the focus has been mainly on both the active materials such as perovskite, ETL and HTM layers and their low temperature processing on conducting flexible substrates such as polyethylene terephthalate (PET), polyethersulfone (PES), polyethylene naphthalate (PEN) or polycarbonate (PC).[218,219] On the other hand, the focus of patents on LT-PSCs has mostly been on low temperature processing primarily on rigid glass substrates.

13.2. Publication trends in PSCs and f-PSCs

Fig. 10c shows a statistical analysis of PSCs *vs.* f-PSCs (papers published on flexible substrates only with respect to all paper published on PSCs), drawn based on data taken from Scopus (dated 15 March 2016) using key words 'perovskite solar cells' and 'flexible perovskite solar cells or perovskite solar cells AND flexible'. While the former revealed a total of 1602 documents published in PSCs, the latter showed an emerging trend in f-SPCs only after 2013 with a total of 105 documents published so far using flexible substrates. For PSCs, the largest number of documents have been published from China (493) followed by United States (315), South Korea (161), United Kingdom (126), Japan (121), and Switzerland (119) (graph not shown). The trends for f-PSCs are nearly the same except that Germany replaces Switzerland for 6th place (China 40, USA 23, S, Korea 17, UK 7, Japan 5 and Germany 4). The statistics show a fair distribution of research activities spread across the globe. Since high PCE values (15.6%),[57] together with the first reports on flexible modules[108] and stability investigations[102] for f-PSCs have only started to be published very recently, research is likely to trend upwards rapidly over time thereby making this a very interesting area for research.

14. Conclusion and outlook

Perovskite solar cells have attracted huge interest because they are able to combine the benefits of high efficiency and remarkable ease of processing over large areas. Perovskite deposition and synthesis is carried out at low temperatures to convert precursors into its final semiconducting form (<150 °C). Most of the development of this technology has occurred on glass, especially initially, due to some of the other layers requiring high temperatures and growing reproducibly high quality films on different substrates (*e.g.* PET/ITO). Research however has been accelerating in the flexible arena and in a short time flexible PSCs have achieved remarkable milestones. For example, PCEs of 15.4–15.6%,[57] and 11.0%[124] have already been obtained on a conducting plastic substrates and metal foils respectively. Several TCO-free architectures have demonstrated that the PSC structure is highly flexible. Furthermore, the use of ultrathin PET substrates coupled with a flexible electrode were instrumental in producing a stretchable and ultralight PSC with a very high power per gram ratio of 23 W g^{-1}, a record for PV devices.[132] Moreover, elastic cells based on titanium fiber coil have been demonstrated, allowing the realization of stretchable fabrics made with PSCs.[161]

For the n–i–p architecture with the ETL at the bottom, notable performance has been demonstrated both with ALD, sputtering and with different solution processed ETLs such as TiO_2, ZnO and $ZnSnO_4$ nanoparticles.[55] The development of similar approaches, based on nanoparticle dispersions, should be encouraged also for the HTM processing with a view to improve stability. In the case of p–i–n architecture with the ETL, the use of polymers as extraction layers makes these seem easier to print over larger areas with PCBM strongly limiting the hysteresis effect. More investigations are encouraged in comparing these two architectures both on power conversion efficiency and stability to understand in more depth the pros and cons relating to both.

Besides the positive achievements already demonstrated, like the first rigid module manufactured,[173] the route to a large area production of PSC is still long and presents a series of challenges. Large area techniques need to be adapted for all the layers used in the PSC, without compromising high efficiency.

Perovskite processing might not be the biggest issue in terms of available techniques, since slot-die coating has already demonstrated maintaining a high PCE, especially on glass.[112]

However, the solvents used at this stage are not very compatible with large production volumes and green alternatives are to be sought. Another arena that requires more investigation is the top electrode. If there are no requirements for transparency, *ad hoc* carbon paste might be a low cost and efficient alternative to expensive metals such as gold deposited by vacuum techniques, as already demonstrated on rigid and flexible substrate.[68,110] On the other hand, if a transparent top contact is needed, the use of well-established techniques for TCO deposition or lamination of conductive foils should be further tested in terms of stability and application over larger areas. A more in depth analysis on the pros and cons of vacuum techniques *vs.* solution processing in terms of performance and costs and compatibility with R-2-R processing should be investigated and presented clearly.

The biggest question mark that always remains for photovoltaic technologies (and in general optoelectronic) developed on a flexible transparent substrate is stability. This is due to the fact that common polymer substrates are permeable to ingress of moisture and oxygen. As historically has been the case for other technologies, investigations on degradation and stability have lagged behind those on optimization of device efficiency. However, recently a number of studies have appeared both on analysis of degradation mechanisms and the use of encapsulants. Further work needs to be carried out in this area which is crucial for industrialization. For example, Heliatek uses R-2-R production for their organic photovoltaic devices and encapsulate them with barrier film, then applying them to different surfaces like steel, PVC membrane and concrete or in between glass panes.[86] This shows on the one hand the strong benefits for R-2-R production on plastic but also that much interdisciplinary work needs to be carried out to improve the cost/performance of flexible encapsulation as well as focusing on finding active material alternatives (*e.g.* news perovskites, HTLs, ETLs and contacts) and especially their combination which are inherently more stable to photo-oxidation and more impervious to moisture. Some limitations due to the nature of the substrate itself have also to be overcome. The low temperature ITO itself might be an issue in long term operation of PSC, since some preliminary tests have shown ITO-induced degradation of the perovskite layer.[108] Further studies have to be carried out in order to better understand the compatibility of PSC with this kind of TCO.

Even if there are still several milestones yet to achieve, flexible PSCs have disruptive potential in PV applications, thanks to the low cost and low embedded energy of the materials used and the high device efficiencies. With respect to glass-based counterparts, the use of R2R production can further decrease the cost making this device more attractive for the market. Finally, the flexibility and even the stretchability of these devices pave the way for new applications in portable and lightweight self-powered devices.

Acknowledgements

FDG, TMB thank ''Polo Solare Organico'' Regione Lazio, MIUR ''AQUASOL'' (Celle solari polimeriche processabili da mezzi acquosi: dai materiali ai moduli fotovoltaici) PRIN 2012 (2012A4Z2RY), and FP7 CHEETAH no. 609788 projects for financial support. AF and RJ acknowledge the Ministry of Higher Education Malaysia for research grant FRGS 140126. AF thanks Alexander von Humboldt Foundation for the post-doctoral research fellowship.

References

1 R. Smalley, *Energy & NanoTechnology Conference*, Rice University, 2003.
2 S. Chu and A. Majumdar, *Nature*, 2012, **488**, 294–303.
3 M. Hosenuzzaman, N. A. Rahim, J. Selvaraj, M. Hasanuzzaman, A. B. M. A. Malek and A. Nahar, *Renewable Sustainable Energy Rev.*, 2015, **41**, 284–297.
4 I. E. Agency, IEA: Solar PVs, http://www.iea.org/topics/solarpvandcsp/, accessed 12-12-2013, 2013.
5 A. Whiteman, S. Elsayed, O. L. d'Ortigue, IRENA Renewable Energy Capacity Statistics, 2015, pp.1–44.
6 M. A. Green, *J. Mater. Sci.: Mater. Electron.*, 2007, **18**, 15–19.
7 A. Fakharuddin, R. Jose, T. M. Brown, F. Fabregat-Santiago and J. Bisquert, *Energy Environ. Sci.*, 2014, **7**, 3952–3981.
8 M. Grätzel, *J. Photochem. Photobiol., C*, 2003, **4**, 145–153.
9 G. Li, R. Zhu and Y. Yang, *Nat. Photonics*, 2012, **6**, 153–161.
10 B. Walker, C. Kim and T.-Q. Nguyen, *Chem. Mater.*, 2011, **23**, 470–482.
11 P. REPORT, ed. I. Fraunhofer, ISE Fraunhofer, Germany, 2015, pp. 1–41.
12 M. A. Green, K. Emery, Y. Hishikawa, W. Warta and E. D. Dunlop, *Prog. Photovoltaics*, 2016, **24**, 3–11.
13 Z. M. Beiley and M. D. McGehee, *Energy Environ. Sci.*, 2012, **5**, 9173–9179.
14 pv-magazine.
15 Wikipedia.
16 D. Campisi, D. Morea and E. Farinelli, *International Journal of Energy Sector Management*, 2015, **9**, 156–175.
17 H. Sun, Q. Zhi, Y. Wang, Q. Yao and J. Su, *Appl. Energy*, 2014, **118**, 221–230.
18 T. M. Brown, F. De Rossi, F. Di Giacomo, G. Mincuzzi, V. Zardetto, A. Reale and A. Di Carlo, *J. Mater. Chem. A*, 2014, **2**, 10788–10817.
19 D. Bi, W. Tress, M. I. Dar, P. Gao, J. Luo, C. Renevier, K. Schenk, A. Abate, F. Giordano, J.-P. Correa Baena, J.-D. Decoppet, S. M. Zakeeruddin, M. K. Nazeeruddin, M. Grätzel and A. Hagfeldt, *Sci. Adv.*, 2016, **2**, e1501170.
20 NREL, Best research cell efficiencies, 2015.
21 M. Saliba, S. Orlandi, T. Matsui, S. Aghazada, M. Cavazzini, J.-P. Correa-Baena, P. Gao, R. Scopelliti, E. Mosconi, K.-H. Dahmen, F. De Angelis, A. Abate, A. Hagfeldt, G. Pozzi, M. Graetzel and M. K. Nazeeruddin, *Nature Energy*, 2016, 15017.
22 M. Saliba, T. Matsui, J.-Y. Seo, K. Domanski, J.-P. Correa-Baena, M. K. Nazeeruddin, S. M. Zakeeruddin, W. Tress, A. Abate, A. Hagfeldt and M. Gratzel, *Energy Environ. Sci.*, 2016, **9**, 1989–1997.

23 W. S. Yang, J. H. Noh, N. J. Jeon, Y. C. Kim, S. Ryu, J. Seo and S. I. Seok, *Science*, 2015, **348**, 1234–1237.
24 F. Matteocci, L. Cinà, F. Di Giacomo, S. Razza, A. L. Palma, A. Guidobaldi, A. D'Epifanio, S. Licoccia, T. M. Brown, A. Reale and A. Di Carlo, *Prog. Photovoltaics*, 2014, **24**, 436–445.
25 T. M. Robert Gehlhaar, Cesar Masse de la Huerta, Weiming Qiu, David Cheyns and Tom Aernouts, 2015, 3, http://spie.org/newsroom.
26 W. Qiu, T. Merckx, M. Jaysankar, C. Masse de la Huerta, L. Rakocevic, W. Zhang, U. W. Paetzold, R. Gehlhaar, L. Froyen, J. Poortmans, D. Cheyns, H. J. Snaith and P. Heremans, *Energy Environ. Sci.*, 2016, **9**, 484–489.
27 A. Kojima, K. Teshima, Y. Shirai and T. Miyasaka, *J. Am. Chem. Soc.*, 2009, **131**, 6050–6051.
28 D. B. Mitzi, C. A. Feild, Z. Schlesinger and R. B. Laibowitz, *J. Solid State Chem.*, 1995, **114**, 159–163.
29 I. B. Koutselas, L. Ducasse and G. C. Papavassiliou, *J. Phys.: Condens. Matter*, 1996, **8**, 1217–1227.
30 D. B. Mitzi, K. Chondroudis and C. R. Kagan, *IBM J. Res. Dev.*, 2001, **45**, 29–45.
31 H.-S. Kim, C.-R. Lee, J.-H. Im, K.-B. Lee, T. Moehl, A. Marchioro, S.-J. Moon, R. Humphry-Baker, J.-H. Yum, J. E. Moser, M. Grätzel and N.-G. Park, *Sci. Rep.*, 2012, **2**, 591.
32 M. M. Lee, J. Teuscher, T. Miyasaka, T. N. Murakami and H. J. Snaith, *Science*, 2012, **338**, 643–647.
33 G. E. Eperon, V. M. Burlakov, P. Docampo, A. Goriely and H. J. Snaith, *Adv. Funct. Mater.*, 2013, **24**, 151–157.
34 J. Burschka, N. Pellet, S.-J. Moon, R. Humphry-Baker, P. Gao, M. K. Nazeeruddin and M. Grätzel, *Nature*, 2013, **499**, 316–319.
35 K. Liang, D. B. Mitzi and M. T. Prikas, *Chem. Mater.*, 1998, **10**, 403–411.
36 X. Dong, X. Fang, M. Lv, B. Lin, S. Zhang, J. Ding and N. Yuan, *J. Mater. Chem. A*, 2015, **3**, 5360–5367.
37 Y. Han, S. Meyer, Y. Dkhissi, K. Weber, J. M. Pringle, U. Bach, L. Spiccia and Y. B. Cheng, *J. Mater. Chem. A*, 2015, **3**, 8139–8147.
38 J. Yang, B. D. Siempelkamp, D. Liu and T. L. Kelly, *ACS Nano*, 2015, **9**, 1955–1963.
39 T. Leijtens, G. E. Eperon, S. Pathak, A. Abate, M. M. Lee and H. J. Snaith, *Nat. Commun.*, 2013, **4**, 2885.
40 L. K. Ono, S. R. Raga, S. Wang, Y. Kato and Y. Qi, *J. Mater. Chem. A*, 2015, **3**, 9074–9080.
41 S. N. Habisreutinger, T. Leijtens, G. E. Eperon, S. D. Stranks, R. J. Nicholas and H. J. Snaith, *Nano Lett.*, 2014, **14**, 5561–5568.
42 Oxford-PV, 2015.
43 Y. Galagan, E. W. C. Coenen, W. J. H. Verhees and R. Andriessen, *J. Mater. Chem. A*, 2016, **4**, 5700–5705.
44 S. Razza, F. Di Giacomo, F. Matteocci, L. Cinà, A. L. Palma, S. Casaluci, P. Cameron, A. D'Epifanio, S. Licoccia, A. Reale, T. M. Brown and A. Di Carlo, *J. Power Sources*, 2015, **277**, 286–291.
45 M. A. Green, A. Ho-Baillie and H. J. Snaith, *Nat. Photonics*, 2014, **8**, 506–514.
46 R. Asadpour, R. V. K. Chavali, M. Ryyan Khan and M. A. Alam, *Appl. Phys. Lett.*, 2015, **106**, 243902.
47 C. D. Bailie, M. G. Christoforo, J. P. Mailoa, A. R. Bowring, E. L. Unger, W. H. Nguyen, J. Burschka, N. Pellet, J. Z. Lee, M. Grätzel, R. Noufi, T. Buonassisi, A. Salleo and M. D. McGehee, *Energy Environ. Sci.*, 2015, **8**, 956–963.
48 C. D. Bailie and M. D. McGehee, *MRS Bull.*, 2015, **40**, 681–685.
49 P. Löper, S. J. Moon, S. Martín De Nicolas, B. Niesen, M. Ledinsky, S. Nicolay, J. Bailat, J. H. Yum, S. De Wolf and C. Ballif, *Phys. Chem. Chem. Phys.*, 2015, **17**, 1619–1629.
50 T. Todorov, T. Gershon, O. Gunawan, Y. S. Lee, C. Sturdevant, L. Y. Chang and S. Guha, *Adv. Energy Mater.*, 2015, **5**, DOI: 10.1002/aenm.201500799.
51 Y. Yang Michael, Q. Chen, Y. T. Hsieh, T. B. Song, N. D. Marco, H. Zhou and Y. Yang, *ACS Nano*, 2015, **9**, 7714–7721.
52 D. Liu and T. L. Kelly, *Nat. Photonics*, 2014, **8**, 133–138.
53 V. Zardetto, T. M. Brown, A. Reale and A. Di Carlo, *J. Polym. Sci., Part B: Polym. Phys.*, 2011, **49**, 638–648.
54 G. Hashmi, K. Miettunen, T. Peltola, J. Halme, I. Asghar, K. Aitola, M. Toivola and P. Lund, *Renewable Sustainable Energy Rev.*, 2011, **15**, 3717–3732.
55 S. S. Shin, W. S. Yang, J. H. Noh, J. H. Suk, N. J. Jeon, J. H. Park, J. S. Kim, W. M. Seong and S. I. Seok, *Nat. Commun.*, 2015, **6**, 7410.
56 Y. Li, L. Meng, Y. Yang, G. Xu, Z. Hong, Q. Chen, J. You, G. Li, Y. Yang and Y. Li, *Nat. Commun.*, 2016, **7**, 10214.
57 J. H. Heo, M. H. Lee, H. J. Han, B. R. Patil, J. S. Yu and S. H. Im, *J. Mater. Chem. A*, 2016, **4**, 1572–1578.
58 K. Kawashima, Y. Tamai, H. Ohkita, I. Osaka and K. Takimiya, *Nat. Commun.*, 2015, **6**, 10085.
59 K. Kakiage, Y. Aoyama, T. Yano, K. Oya, J.-i. Fujisawa and M. Hanaya, *Chem. Commun.*, 2015, **51**, 15894–15897.
60 V. Zardetto, G. Mincuzzi, F. De Rossi, F. Di Giacomo, A. Reale, A. Di Carlo and T. M. Brown, *Appl. Energy*, 2014, **113**, 1155–1161.
61 P. P. Boix, K. Nonomura, N. Mathews and S. G. Mhaisalkar, *Mater. Today*, 2014, **17**, 16–23.
62 W. H. Zhang and B. Cai, *Chin. Sci. Bull.*, 2014, **59**, 2092–2101.
63 T.-B. Song, Q. Chen, H.-P. Zhou, C. Jiang, H.-H. Wang, Y. Yang, Y. Liu and J. You, *J. Mater. Chem. A*, 2015, **3**, 9032–9050.
64 N. Sai, B. Meyer and D. Vanderbilt, *Phys. Rev. Lett.*, 2000, **84**, 5636–5639.
65 Q. Dong, Y. Fang, Y. Shao, P. Mulligan, J. Qiu, L. Cao and J. Huang, *Science*, 2015, **347**, 967–970.
66 Y. Shi, Y. Xing, Y. Li, Q. Dong, K. Wang, Y. Du, X. Bai, S. Wang, Z. Chen and T. Ma, *J. Phys. Chem. C*, 2015, **119**, 15868–15873.
67 D. T. Moore, H. Sai, K. W. Tan, D.-M. Smilgies, W. Zhang, H. J. Snaith, U. Wiesner and L. A. Estroff, *J. Am. Chem. Soc.*, 2015, **137**, 2350–2358.
68 A. Mei, X. Li, L. Liu, Z. Ku, T. Liu, Y. Rong, M. Xu, M. Hu, J. Chen, Y. Yang, M. Gratzel and H. Han, *Science*, 2014, **345**, 295–298.

69 M. Paggi, I. Berardone, A. Infuso and M. Corrado, *Sci. Rep.*, 2014, **4**, 4506.
70 P. J. Verlinden, A. W. Blakers, K. J. Weber, J. Babaei, V. Everett, M. J. Kerr, M. F. Stuckings, D. Gordeev and M. J. Stocks, *Sol. Energy Mater. Sol. Cells*, 2006, **90**, 3422–3430.
71 A. W. Blakers and T. Armour, *Sol. Energy Mater. Sol. Cells*, 2009, **93**, 1440–1443.
72 B. M. Kayes, H. Nie, R. Twist, S. G. Spruytte, F. Reinhardt, I. C. Kizilyalli and G. S. Higashi, in Photovoltaic Specialists Conference (PVSC), 2011 37th IEEE, 2011, pp. 000004–000008.
73 G. J. Bauhuis, J. J. Schermer, P. Mulder, M. M. A. J. Voncken and P. K. Larsen, *Sol. Energy Mater. Sol. Cells*, 2004, **83**, 81–90.
74 R. M. Swanson, *Prog. Photovoltaics*, 2000, **8**, 93–111.
75 B. Yan, G. Yue, J. Yang and S. Guha, in Active-Matrix Flatpanel Displays and Devices (AM-FPD), 2012 19th International Workshop on, 2012, pp. 67–70.
76 H. P. Mahabaduge, W. L. Rance, J. M. Burst, M. O. Reese, D. M. Meysing, C. A. Wolden, J. Li, J. D. Beach, T. A. Gessert, W. K. Metzger, S. Garner and T. M. Barnes, *Appl. Phys. Lett.*, 2015, **106**, 133501.
77 L. Kranz, S. Buecheler and A. N. Tiwari, *Sol. Energy Mater. Sol. Cells*, 2013, **119**, 278–280.
78 L. Kranz, C. Gretener, J. Perrenoud, R. Schmitt, F. Pianezzi, F. La Mattina, P. Blösch, E. Cheah, A. Chirilă, C. M. Fella, H. Hagendorfer, T. Jäger, S. Nishiwaki, A. R. Uhl, S. Buecheler and A. N. Tiwari, *Nat. Commun.*, 2013, **4**, 2306.
79 P. Reinhard, A. Chirila, F. Pianezzi, S. Nishiwaki, S. Buecheler and A. N. Tiwari, in *Active-Matrix Flatpanel Displays and Devices (AM-FPD), 2013 Twentieth International Workshop on*, 2013, pp. 79–82.
80 T. Yamaguchi, N. Tobe, D. Matsumoto, T. Nagai and H. Arakawa, *Sol. Energy Mater. Sol. Cells*, 2010, **94**, 812–816.
81 J. H. Park, Y. Jun, H.-G. Yun, S.-Y. Lee and M. G. Kang, *J. Electrochem. Soc.*, 2008, **155**, F145–F149.
82 F. De Rossi, T. Pontecorvo and T. M. Brown, *Appl. Energy*, 2015, **156**, 413–422.
83 F. C. Krebs, *Sol. Energy Mater. Sol. Cells*, 2009, **93**, 1636–1641.
84 D. J. Lipomi, B. C. K. Tee, M. Vosgueritchian and Z. Bao, *Adv. Mater.*, 2011, **23**, 1771–1775.
85 M. Kaltenbrunner, G. Adam, E. D. Glowacki, M. Drack, R. Schwodiauer, L. Leonat, D. H. Apaydin, H. Groiss, M. C. Scharber, M. S. White, N. S. Sariciftci and S. Bauer, *Nat. Mater.*, 2015, **14**, 1032–1039.
86 Heliatek, Personal communication and ''Heliatek sets new Organic Photovoltaic world record efficiency of 13.2%'', http://www.heliatek.com/en/press/press-releases, accessed June 2016.
87 F. Fu, T. Feurer, T. Jager, E. Avancini, B. Bissig, S. Yoon, S. Buecheler and A. N. Tiwari, *Nat. Commun.*, 2015, **6**, 8932.
88 M. Dianetti, F. Di Giacomo, G. Polino, C. Ciceroni, A. Liscio, A. D'Epifanio, S. Licoccia, T. M. Brown, A. Di Carlo and F. Brunetti, *Sol. Energy Mater. Sol. Cells*, 2015, **140**, 150–157.
89 F. C. Krebs, M. Jørgensen, K. Norrman, O. Hagemann, J. Alstrup, T. D. Nielsen, J. Fyenbo, K. Larsen and J. Kristensen, *Sol. Energy Mater. Sol. Cells*, 2009, **93**, 422–441.
90 S. Bonthu, G. Lingamallu and S. P. Singh, *Chem. Commun.*, 2015, **51**, 14696–14707.
91 H. Zhou, Q. Chen, G. Li, S. Luo, T.-b. Song, H.-S. Duan, Z. Hong, J. You, Y. Liu and Y. Yang, *Science*, 2014, **345**, 542–546.
92 Y. Dkhissi, F. Huang, S. Rubanov, M. Xiao, U. Bach, L. Spiccia, R. A. Caruso and Y.-B. Cheng, *J. Power Sources*, 2015, **278**, 325–331.
93 C. Roldán-Carmona, O. Malinkiewicz, A. Soriano, G. Mínguez Espallargas, A. Garcia, P. Reinecke, T. Kroyer, M. I. Dar, M. K. Nazeeruddin and H. J. Bolink, *Energy Environ. Sci.*, 2014, **7**, 994.
94 B. J. Kim, D. H. Kim, Y. Y. Lee, H. W. Shin, G. S. Han, J. S. Hong, K. Mahmood, T. K. Ahn, Y. C. Joo, K. S. Hong, N. G. Park, S. Lee and H. S. Jung, *Energy Environ. Sci.*, 2015, **8**, 916–921.
95 P. Docampo, J. M. Ball, M. Darwich, G. E. Eperon and H. J. Snaith, *Nat. Commun.*, 2013, **4**, 2761.
96 X. Xu, Q. Chen, Z. Hong, H. Zhou, Z. Liu, W.-H. Chang, P. Sun, H. Chen, N. D. Marco, M. Wang and Y. Yang, *Nano Lett.*, 2015, **15**, 6514–6520.
97 D. Liu, M. K. Gangishetty and T. L. Kelly, *J. Mater. Chem. A*, 2014, **2**, 19873–19881.
98 Y. Zhang, M. Liu, G. E. Eperon, T. Leijtens, D. P. McMeekin, M. Saliba, W. Zhang, M. De Bastiani, A. Petrozza, L. Herz, M. B. Johnston, H. Lin and H. Snaith, *Mater. Horiz.*, 2015, **2**, 315–322.
99 D. Yang, R. Yang, J. Zhang, Z. Yang, S. Liu and C. Li, *Energy Environ. Sci.*, 2015, **8**, 3208–3214.
100 W. Qiu, U. W. Paetzold, R. Gehlhaar, V. Smirnov, H.-G. Boyen, J. G. Tait, B. Conings, W. Zhang, C. Nielsen, I. McCulloch, L. Froyen, P. Heremans and D. Cheyns, *J. Mater. Chem. A*, 2015, **3**, 22824–22829.
101 M. M. Tavakoli, K.-H. Tsui, S.-F. Leung, Q. Zhang, J. He, Y. Yao, D. Li and Z. Fan, *ACS Nano*, 2015, **9**, 10287–10295.
102 H. C. Weerasinghe, Y. Dkhissi, A. D. Scully, R. A. Caruso and Y.-B. Cheng, *Nano Energy*, 2015, **18**, 118–125.
103 M. M. Tavakoli, Q. Lin, S.-F. Leung, G. C. Lui, H. Lu, L. Li, B. Xiang and Z. Fan, *Nanoscale*, 2016, **8**, 4276–4283.
104 S. Ryu, J. Seo, S. S. Shin, Y. C. Kim, N. J. Jeon, J. H. Noh and S. I. Seok, *J. Mater. Chem. A*, 2015, **3**, 3271–3275.
105 S. Ameen, M. S. Akhtar, H.-K. Seo, M. K. Nazeeruddin and H.-S. Shin, *J. Phys. Chem. C*, 2015, **119**, 10379–10390.
106 S. Das, B. Yang, G. Gu, P. C. Joshi, I. N. Ivanov, C. M. Rouleau, T. Aytug, D. B. Geohegan and K. Xiao, *ACS Photonics*, 2015, **2**, 680–686.
107 S. Ameen, M. S. Akhtar, H.-K. Seo, N. Mohammad K. and H.-S. Shin, *Dalton Trans.*, 2015, **44**, 6439–6448.
108 F. Di Giacomo, V. Zardetto, A. D'Epifanio, S. Pescetelli, F. Matteocci, S. Razza, A. Di Carlo, S. Licoccia, W. M. M. Kessels, M. Creatore and T. M. Brown, *Adv. Energy Mater.*, 2015, **5**, DOI: 10.1002/aenm.201401808.
109 T. M. Schmidt, T. T. Larsen-olsen, J. E. Carlé, D. Angmo and F. C. Krebs, *Adv. Energy Mater.*, 2015, **5**, 1500569.

110 H. Zhou, Y. Shi, K. Wang, Q. Dong, X. Bai, Y. Xing, Y. Du and T. Ma, *J. Phys. Chem. C*, 2015, **119**, 4600–4605.
111 M. H. Kumar, N. Yantara, S. Dharani, M. Graetzel, S. Mhaisalkar, P. P. Boix and N. Mathews, *Chem. Commun.*, 2013, **49**, 11089–11091.
112 K. Hwang, Y.-S. Jung, Y.-J. Heo, F. H. Scholes, S. E. Watkins, J. Subbiah, D. J. Jones, D.-Y. Kim and D. Vak, *Adv. Mater.*, 2015, **27**, 1241–1247.
113 A. Fakharuddin, I. Ahmed, Z. Khalidin, M. M. Yusoff and R. Jose, *Appl. Phys. Lett.*, 2014, **104**, 053905.
114 T. Dittrich, E. A. Lebedev and J. Weidmann, *Phys. Status Solidi A*, 1998, **165**, R5–R6.
115 E. M. C. Fortunato, P. M. C. Barquinha, A. C. M. B. G. Pimentel, A. M. F. Gonalves, A. N. J. S. Marques, R. F. P. Martins and L. M. N. Pereira, *Appl. Phys. Lett.*, 2004, **85**, 2541.
116 Q. Wali, A. Fakharuddin, I. Ahmed, M. H. Ab Rahim, J. Ismail and R. Jose, *J. Mater. Chem. A*, 2014, **2**, 17427–17434.
117 Q. Wali, A. Fakharuddin, A. Yasin, M. H. Ab Rahim, J. Ismail and R. Jose, *J. Alloys Compd.*, 2015, **646**, 32–39.
118 Q. Wali, A. Fakharuddin and R. Jose, *J. Power Sources*, 2015, **293**, 1039–1052.
119 S. K. Hau, H.-L. Yip, N. S. Baek, J. Zou, K. O'Malley and A. K.-Y. Jen, *Appl. Phys. Lett.*, 2008, **92**, 253301.
120 Y. Yang, J. You, Z. Hong, Q. Chen, M. Cai, T. B. Song, C. C. Chen, S. Lu, Y. Liu and H. Zhou, *ACS Nano*, 2014, **8**, 1674–1680.
121 J. Yang, B. D. Siempelkamp, E. Mosconi, F. De Angelis and T. L. Kelly, *Chem. Mater.*, 2015, **27**, 4229–4236.
122 X. Dong, H. Hu, B. Lin, J. Ding and N. Yuan, *Chem. Commun.*, 2014, **50**, 14405–14408.
123 F. Matteocci, G. Mincuzzi, F. Giordano, A. Capasso, E. Artuso, C. Barolo, G. Viscardi, T. M. Brown, A. Reale and A. Di Carlo, *Org. Electron.*, 2013, **14**, 1882–1890.
124 M. Lee, Y. Jo, D. S. Kim, H. Y. Jeong and Y. Jun, *J. Mater. Chem. A*, 2015, **3**, 14592–14597.
125 V. Zardetto, F. Di Giacomo, D. Garcia-Alonso, W. Keuning, M. Creatore, C. Mazzuca, A. Reale, A. Di Carlo and T. M. Brown, *Adv. Energy Mater.*, 2013, **3**, 1292–1298.
126 A. Yella, L. P. Heiniger, P. Gao, M. K. Nazeeruddin and M. Grätzel, *Nano Lett.*, 2014, **14**, 2591–2596.
127 A. Kogo, Y. Sanehira, M. Ikegami and T. Miyasaka, *J. Mater. Chem. A*, 2015, **3**, 20952–20957.
128 B. Conings, L. Baeten, T. Jacobs, R. Dera, J. D'Haen, J. Manca and H.-G. Boyen, *APL Mater.*, 2014, **2**, 081505.
129 H. Zhang, J. Cheng, F. Lin, H. He, J. Mao, K. S. Wong, A. K. Y. Jen and W. C. H. Choy, *ACS Nano*, 2016, **10**, 1503–1511.
130 K. Yao, X. Wang, Y.-X. Xu and F. Li, *Nano Energy*, 2015, **18**, 165–175.
131 X. Yin, P. Chen, M. Que, Y. Xing, W. Que, C. Niu and J. Shao, *ACS Nano*, 2016, **10**, 3630–3636.
132 M. Kaltenbrunner, G. Adam, E. D. Glowacki, M. Drack, R. Schwodiauer, L. Leonat, D. H. Apaydin, H. Groiss, M. C. Scharber, M. S. White, N. S. Sariciftci and S. Bauer, *Nat. Mater.*, 2015, **14**, 1032–1039.
133 Y. Chen, T. Chen and L. Dai, *Adv. Mater.*, 2015, **27**, 1053–1059.
134 X. Bao, Q. Zhu, M. Qiu, A. Yang, Y. Wang, D. Zhu, J. Wang and R. Yang, *J. Mater. Chem. A*, 2015, **3**, 19294–19298.
135 J. W. Jung, S. T. Williams and A. K.-Y. Jen, *RSC Adv.*, 2014, **4**, 62971–62977.
136 Y. Chen, Y. Zhao and Z. Liang, *Chem. Mater.*, 2015, **27**, 1448–1451.
137 K. G. Lim, H. B. Kim, J. Jeong, H. Kim, J. Y. Kim and T. W. Lee, *Advanced Materials*, 2014, pp. 1–6.
138 Z. Yang, C.-C. Chueh, F. Zuo, J. H. Kim, P.-W. Liang and A. K. Y. Jen, *Adv. Energy Mater.*, 2015, **5**, DOI: 10.1002/aenm.201500328.
139 Z. Gu, L. Zuo, T. T. Larsen-Olsen, T. Ye, G. Wu, F. C. Krebs and H. Chen, *J. Mater. Chem. A*, 2015, **3**, 24254–24260.
140 Y. F. Chiang, J. Y. Jeng, M. H. Lee, S. R. Peng, P. Chen, T. F. Guo, T. C. Wen, Y. J. Hsu and C. M. Hsu, *Phys. Chem. Chem. Phys.*, 2014, **16**, 6033–6040.
141 T. M. Brown, J. S. Kim, R. H. Friend, F. Cacialli, R. Daik and W. J. Feast, *Appl. Phys. Lett.*, 1999, **75**, 1679–1681.
142 Y. He and Y. Li, *Phys. Chem. Chem. Phys.*, 2011, **13**, 1970–1983.
143 W. Yan, Y. Li, Y. Li, S. Ye, Z. Liu, S. Wang, Z. Bian and C. Huang, *Nano Res.*, 2015, **8**, 2474.
144 K. Wojciechowski, T. Leijtens, S. Spirova, C. Schlueter, M. Hoerantner, J. T.-W. Wang, C.-Z. Li, A. K.-Y. Jen, T.-L. Lee and H. J. Snaith, *J. Phys. Chem. Lett.*, 2015, **6**, 2399–2405.
145 Y. Shao, Z. Xiao, C. Bi, Y. Yuan and J. Huang, *Nat. Commun.*, 2014, **5**, 5784.
146 C. Bi, Q. Wang, Y. Shao, Y. Yuan, Z. Xiao and J. Huang, *Nat. Commun.*, 2015, **6**, 7747.
147 F. Hou, Z. Su, F. Jin, X. Yan, L. Wang, H. Zhao, J. Zhu, B. Chu and W. Li, *Nanoscale*, 2015, **7**, 9427–9432.
148 W. Qiu, M. Buffière, G. Brammertz, U. W. Paetzold, L. Froyen, P. Heremans and D. Cheyns, *Org. Electron.*, 2015, **26**, 30–35.
149 S. Chavhan, O. Miguel, H. J. Grande, V. Gonzalez-Pedro, R. S. Sánchez, E. M. Barea, I. Mora-Seró and R. Tena-Zaera, *J. Mater. Chem. A*, 2014, **2**, 12754–12760.
150 S. Ye, W. Sun, Y. Li, W. Yan, H. Peng, Z. Bian, Z. Liu and C. Huang, *Nano Lett.*, 2015, **15**, 3723–3728.
151 C. Zuo and L. Ding, *Small*, 2015, **11**, 5528–5532.
152 M. Park, H. J. Kim, I. Jeong, J. Lee, H. Lee, H. J. Son, D. E. Kim and M. J. Ko, *Adv. Energy Mater.*, 2015, **5**, DOI: 10.1002/aenm.201501406.
153 K. Sun, P. Li, Y. Xia, J. Chang and J. Ouyang, *ACS Appl. Mater. Interfaces*, 2015, 15314–15320.
154 K. Poorkazem, D. Liu and T. L. Kelly, *J. Mater. Chem. A*, 2015, **3**, 9241–9248.
155 I. Jeon, T. Chiba, C. Delacou, Y. Guo, A. Kaskela, O. Reynaud, E. I. Kauppinen, S. Maruyama and Y. Matsuo, *Nano Lett.*, 2015, **15**, 6665–6671.
156 M. Sessolo and H. J. Bolink, *Nat. Mater.*, 2015, **14**, 964–966.
157 Y. Xiao, G. Han, H. Zhou and J. Wu, *RSC Adv.*, 2016, **6**, 2778–2784.

158 J. Troughton, D. Bryant, K. Wojciechowski, M. J. Carnie, H. Snaith, D. A. Worsley and T. M. Watson, *J. Mater. Chem. A*, 2015, **3**, 9141–9145.
159 X. Wang, Z. Li, W. Xu, S. A. Kulkarni, S. K. Batabyal, S. Zhang, A. Cao and L. H. Wong, *Nano Energy*, 2015, **11**, 728–735.
160 M. Lee, Y. Ko, B. K. Min and Y. Jun, *ChemSusChem*, 2016, **9**, 31–35.
161 J. Deng, L. Qiu, X. Lu, Z. Yang, G. Guan, Z. Zhang and H. Peng, *J. Mater. Chem. A*, 2015, **3**, 21070–21076.
162 M. Lee, Y. Ko and Y. Jun, *J. Mater. Chem. A*, 2015, **3**, 4129–4133.
163 S. He, L. Qiu, X. Fang, G. Guan, P. Chen, Z. Zhang and H. Peng, *J. Mater. Chem. A*, 2015, **3**, 9406–9410.
164 L. Qiu, J. Deng, X. Lu, Z. Yang and H. Peng, *Angew. Chem., Int. Ed.*, 2014, 2–6.
165 F. Kessler and D. Rudmann, *Sol. Energy*, 2004, **77**, 685–695.
166 J. Ryan, *Methods of scoring for fabricating interconnected photovoltaic cells*, US 7932464 B2, 2011.
167 D. Bryant, P. Greenwood, J. Troughton, M. Wijdekop, M. Carnie, M. Davies, K. Wojciechowski, H. J. Snaith, T. Watson and D. Worsley, *Adv. Mater.*, 2014, **26**, 7499–7504.
168 C.-Y. Chang, K.-T. Lee, W.-K. Huang, H.-Y. Siao and Y.-C. Chang, *Chem. Mater.*, 2015, **27**, 5122–5130.
169 C. S. Rustomji, C. J. Frandsen, S. Jin and M. J. Tauber, *J. Phys. Chem. B*, 2010, **114**, 14537–14543.
170 M. G. Kang and L. J. Guo, *Adv. Mater.*, 2007, **19**, 1391–1396.
171 S.-J. Moon, J.-H. Yum, L. Lofgren, A. Walter, L. Sansonnens, M. Benkhaira, S. Nicolay, J. Bailat and C. Ballif, *IEEE J. Photovolt.*, 2015, **5**, 1087–1092.
172 G. Mincuzzi, A. L. Palma, A. DiCarlo and T. M. Brown, *ChemElectroChem*, 2016, **3**, 9–30.
173 F. Matteocci, S. Razza, F. Di Giacomo, S. Casaluci, G. Mincuzzi, T. M. Brown, A. D'Epifanio, S. Licoccia and A. Di Carlo, *Phys. Chem. Chem. Phys.*, 2014, **16**, 3918–3923.
174 J. Seo, S. Park, Y. Chan Kim, N. J. Jeon, J. H. Noh, S. C. Yoon and S. I. Seok, *Energy Environ. Sci.*, 2014, **7**, 2642.
175 J. H. Heo, H. J. Han, D. Kim, T. K. Ahn and S. H. Im, *Energy Environ. Sci.*, 2015, **8**, 1602–1608.
176 D. Vak, K. Hwang, A. Faulks, Y. S. Jung, N. Clark, D. Y. Kim, G. J. Wilson and S. E. Watkins, *Adv. Energy Mater.*, 2015, **5**, DOI: 10.1002/aenm.201401539.
177 F. C. Krebs, *Sol. Energy Mater. Sol. Cells*, 2009, **93**, 394–412.
178 F. C. Krebs, T. Tromholt and M. Jorgensen, *Nanoscale*, 2010, **2**, 873–886.
179 A. T. Barrows, A. J. Pearson, C. K. Kwak, A. D. F. Dunbar, A. R. Buckley and D. G. Lidzey, *Energy Environ. Sci.*, 2014, **7**, 2944–2950.
180 K. Mahmood, B. S. Swain and H. S. Jung, *Nanoscale*, 2014, **6**, 9127–9138.
181 Z. Wei, H. Chen, K. Yan and S. Yang, *Angew. Chem., Int. Ed.*, 2014, **53**, 13239–13243.
182 Z. Yang, C. C. Chueh, F. Zuo, J. H. Kim, P. W. Liang and A. K. Y. Jen, *Adv. Energy Mater.*, 2015, **5**.
183 S. Casaluci, L. Cinà, A. Pockett, P. S. Kubiak, R. G. Niemann, A. Reale, A. Di Carlo and P. J. Cameron, *J. Power Sources*, 2015, **297**, 504–510.
184 A. Fakharuddin, A. L. Palma, F. Di Giacomo, S. Casaluci, F. Matteocci, Q. Wali, M. Rauf, A. Di Carlo, T. M. Brown and R. Jose, *Nanotechnology*, 2015, **26**, 494002.
185 J. Troughton, C. Charbonneau, M. J. Carnie, M. L. Davies, D. A. Worsley and T. M. Watson, *J. Mater. Chem. A*, 2015, **3**, 9123–9127.
186 J. Troughton, M. J. Carnie, M. L. Davies, C. Charbonneau, E. H. Jewell, D. A. Worsley and T. M. Watson, *J. Mater. Chem. A*, 2016, **4**, 3471–3476.
187 F. C. Krebs, J. Fyenbo and M. Jorgensen, *J. Mater. Chem.*, 2010, **20**, 8994–9001.
188 F. C. Krebs, *Sol. Energy Mater. Sol. Cells*, 2009, **93**, 465–475.
189 M. M. Voigt, R. C. I. Mackenzie, C. P. Yau, P. Atienzar, J. Dane, P. E. Keivanidis, D. D. C. Bradley and J. Nelson, *Sol. Energy Mater. Sol. Cells*, 2011, **95**, 731–734.
190 R. Roesch, T. Faber, E. Von Hauff, T. M. Brown, M. Lira-Cantu and H. Hoppe, *Adv. Energy Mater.*, 2015, **5**, DOI: 10.1002/aenm.201501407.
191 T. Leijtens, G. E. Eperon, N. K. Noel, S. N. Habisreutinger, A. Petrozza and H. J. Snaith, *Adv. Energy Mater.*, 2015, **5**, DOI: 10.1002/aenm.201500963..
192 A. Fakharuddin, F. Di Giacomo, I. Ahmed, Q. Wali, T. M. Brown and R. Jose, *J. Power Sources*, 2015, **283**, 61–67.
193 A. Fakharuddin, F. Di Giacomo, A. L. Palma, F. Matteocci, I. Ahmed, S. Razza, A. D'Epifanio, S. Licoccia, J. Ismail, A. Di Carlo, T. M. Brown and R. Jose, *ACS Nano*, 2015, **9**, 8420–8429.
194 G. Niu, X. Guo and L. Wang, *J. Mater. Chem. A*, 2015, **3**, 8970–8980.
195 N. A. Manshor, Q. Wali, K. K. Wong, S. K. Muzakir, A. Fakharuddin, L. Schmidt-Mende and R. Jose, *Phys. Chem. Chem. Phys.*, 2016, **18**, 21629–21639.
196 T. A. Berhe, W.-n. Su, C.-H. Chen, C.-J. Pan, J. Cheng, H.-M. Chen, M.-c. Tsai, L.-Y. Chen, A. A. Dubale and B. J. Hwang, *Energy Environ. Sci.*, 2015, **9**, 323–356.
197 Y. Zhang, Z. Yao, S. Lin, J. Li and H. Lin, *Acta Chim. Sin.*, 2015, **73**, 219–224.
198 C. Zhao, B. Chen, X. Qiao, L. Luan, K. Lu and B. Hu, *Adv. Energy Mater.*, 2015, **5**, DOI: 10.1002/aenm.201500279.
199 O. Almora, I. Zarazua, E. Mas-Marza, I. Mora-Sero, J. Bisquert and G. Garcia-Belmonte, *J. Phys. Chem. Lett.*, 2015, **6**, 1645–1652.
200 R. S. Sanchez, V. Gonzalez-Pedro, J. W. Lee, N. G. Park, Y. S. Kang, I. Mora-Sero and J. Bisquert, *J. Phys. Chem. Lett.*, 2014, **5**, 2357–2363.
201 G. Dennler, C. Lungenschmied, H. Neugebauer, N. S. Sariciftci, M. Latrèche, G. Czeremuszkin and M. R. Wertheimer, *Thin Solid Films*, 2006, **511–512**, 349–353.
202 F. De Rossi, G. Mincuzzi, F. Di Giacomo, J. Fahlteich, S. Amberg-Schwab, K. Noller and T. M. Brown, *Energy Technol.*, 2016, DOI: 10.1002/ente.201600244.
203 K. Yan, M. Long, T. Zhang, Z. Wei, H. Chen, S. Yang and J. Xu, *J. Am. Chem. Soc.*, 2015, **137**, 4460–4468.
204 Alibaba, plastic rolls for lamination and encapsulation, Accessed 15/3/2016, March 2016.
205 H. J. Snaith, MRS 2014 plenary talk-F14-Symposium X, http://www.youtube.com/watch?v=wJE8Q7Ndzaw, accessed on June 2016.

206 J. Kalowekamo and E. Baker, *Sol. Energy*, 2009, **83**, 1224–1231.
207 T. Meyer, M. Scott, A. Azam, D. Martineau, F. Oswald, S. Narbey, G. Laporte, R. Cisneros, G. Tregnano and A. Meyer, *CleanTechDay 3rd Generation Photovoltaics*, CSEM, Basel, 2009.
208 I. R. E. Agency, 2012.
209 C.-Y. Chen, J.-H. Chang, K.-M. Chiang, H.-L. Lin, S.-Y. Hsiao and H.-W. Lin, *Adv. Funct. Mater.*, 2015, **25**, 7064–7070.
210 R. Steim, T. Ameri, P. Schilinsky, C. Waldauf, G. Dennler, M. Scharber and C. J. Brabec, *Sol. Energy Mater. Sol. Cells*, 2011, **95**, 3256–3261.
211 C.-Y. Chen, J.-H. Chang, K.-M. Chiang, H.-L. Lin, S.-Y. Hsiao and H.-W. Lin, *Adv. Funct. Mater.*, 2015, **25**, 7064–7070.
212 F. Di Giacomo, V. Zardetto, G. Lucarelli, L. Cinà, A. Di Carlo, M. Creatore and T. M. Brown, *Nano Energy*, 2016, accepted.
213 G. Lucarelli, F. Di Giacomo, V. Zardetto, M. Creatore and T. M. Brown, *Nano Res.*, 2016, under review.
214 L. Serrano-Lujan, N. Espinosa, T. T. Larsen-Olsen, J. Abad, A. Urbina and F. C. Krebs, *Adv. Energy Mater.*, 2015, **5**, DOI: 10.1002/aenm.201501119.
215 N. Espinosa, L. Serrano-Luján, A. Urbina and F. C. Krebs, *Sol. Energy Mater. Sol. Cells*, 2015, **137**, 303–310.
216 F. Hao, C. C. Stoumpos, D. H. Cao, R. P. H. Chang and M. G. Kanatzidis, *Nat. Photonics*, 2014, **8**, 489–494.
217 Directive 2011/65/EU of the European Parliment, 2011.
218 T. F. Guo, J. Y. Jeng, Y. F. Chiang, M. H. Lee and C. Y. Chen, US 20140332078 A1, 2014.
219 S. Zhan, L. Yang and L. Xin, CN 103400697 A, 2013.